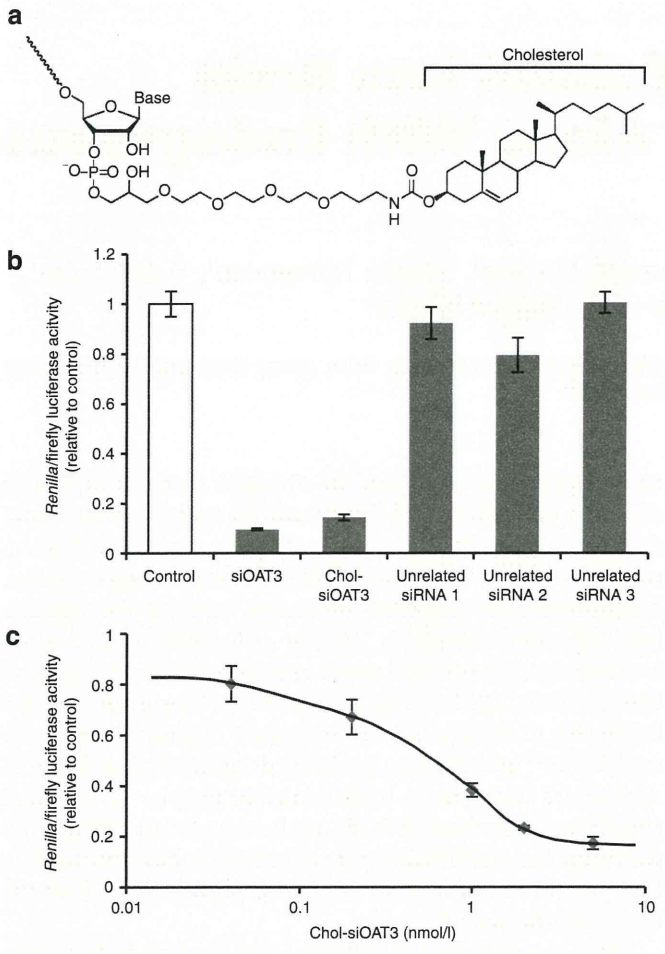

Figure 1 Design of Chol-siRNA targeting organic anion transporter 3 (*OAT3*) mRNA and its *in vitro* gene silencing effect. (**a**) Chemical structure of cholesterol conjugated to the 3′ end of the sense strand. (**b**) *In vitro* gene silencing effect of cholesterol-conjugated short-interfering RNA (siRNA) targeting *OAT3* mRNA (Chol-siOAT3). Luciferase activity was analyzed 24 hours after transfection of Neuro2a cells with the *Renilla* luciferase-fused *OAT3* expression vector, firefly luciferase expression vector, and either unconjugated siRNA targeting *OAT3* mRNA (siOAT3), Chol-siOAT3, or unrelated siRNA (unrelated siRNAs 1, 2, and 3 represent siRNAs targeting mouse claudin-5, apolipoprotein B, and superoxide dismutase-1, respectively) at the concentration of 5 nmol/l. The data shown are relative to the values of the control group (transfected without siRNA). Data are expressed as mean values ± SEM (n = 3). (**c**) *In vitro* gene silencing effect of Chol-siOAT3. Luciferase activity was analyzed 24 hours after transfection of Neuro2a cells with the *Renilla* luciferase-fused *OAT3* expression vector, firefly luciferase expression vector, and Chol-siOAT3 at different concentrations. Data are expressed as mean values ± SEM (n = 5). siRNA, short-interfering RNA; OAT3, organic anion transporter 3.

brain capillary endothelial volume is <0.1% of total brain[1] and therefore the distribution to the BCECs might be below the detection limit. In the present study, we have used endogenous lipoproteins to develop an *in vivo* delivery system for Chol-siRNA to be taken up into the BCECs.

RESULTS

Design of Chol-siRNA targeting *OAT3* mRNA and its *in vitro* gene silencing effect

We designed a 21/23-mer siRNA to target mouse *organic anion transporter 3* (*OAT3*) mRNA (NM_031194) so that there was an overhang of two nucleotides in the 3′-end of its antisense strand.[16] OAT3 is exclusively expressed at the endothelial cells in the brain and plays an important role in the brain-to-blood efflux transport of uremic toxins and neurotransmitter metabolites.[17] The siRNA sequence was taken from our previous report, which described the selection of a good sequence for the cleavage of *OAT3* mRNA.[11] Chemical modifications such as phosphorothioate linkages and 2′-*O*-methyl sugar modifications were introduced into the nucleotides at the 3′ side of the both strands of siRNA to enhance their resistance towards degradation by exo- and endonucleases.[18] Cholesterol was covalently conjugated to the 3′-end of the sense strand by using a cholesteryl-triethyleneglycol phosphoramidite linker (Chol-siOAT3) (**Figure 1a**).

Because the linker used to conjugate cholesterol was different from the pyrrolidine linker reported earlier,[18] we examined the *in vitro* gene silencing effect of Chol-siOAT3 by cotransfection of cultured mouse neuroblastoma (Neuro2a) cells with a *Renilla* luciferase-fused *OAT3* expression vector and a firefly luciferase expression vector. Chol-siOAT3 at the concentration of 5 nmol/l efficiently inhibited the expression of OAT3 by 86.6% relative to the control luciferase activity, an inhibition that was similar to that achieved by an unconjugated siRNA also targeting *OAT3* mRNA (siOAT3) (**Figure 1b**). The expression of OAT3 was not inhibited by unrelated siRNAs that targeted the mRNA of mouse claudin-5 (NM_013805), mouse apolipoprotein-B (*ApoB*) (NM_009693), or mouse superoxide dismutase-1 (NM_011434). The examination of the silencing effect of Chol-siOAT3 at different concentrations showed that the half maximal inhibitory concentration of Chol-siOAT3 was 0.51 nmol/l (**Figure 1c**). Thus, Chol-siOAT3 was considered to be highly efficient and specific in its cleavage of *OAT3* mRNA.

Ex vivo incorporation of Chol-siOAT3 into extracted endogenous lipoproteins

We investigated the character of endogenous lipoproteins used as vectors for Chol-siOAT3 and optimized the composition of *ex vivo* mixture of endogenous lipoproteins and Chol-siOAT3 for animal experiments. We first obtained endogenous lipoproteins from mouse sera by ultracentrifugation. The endogenous HDL fraction was isolated from the sera of wild-type (WT) mice, whereas the endogenous LDL fraction was collected from the sera of LDL receptor (LDLR)-deficient ($LDLR^{-/-}$) mice[19] because WT mice only had small amounts of LDL in their sera.

An analysis of lipid profiles using high-performance liquid chromatography[20] showed that the HDL fraction contained only HDL-cholesterol, with no cholesterol derived from any other lipoproteins (**Figure 2a**), and that the LDL fraction contained only LDL-cholesterol (**Figure 2b**). Moreover, western blotting revealed a characteristic apolipoprotein profile for each lipoprotein fraction: the HDL fraction contained apolipoprotein A-I (ApoA-I) and no ApoB, whereas the LDL fraction contained ApoB (ApoB-100 and ApoB-48) but no apolipoprotein A-I (**Figure 2c**). These results indicate that endogenous HDL and LDL had been successfully isolated.

Next, we incubated siOAT3 or Chol-siOAT3 with the HDL or LDL fraction *ex vivo* and evaluated the electrophoretic mobility of the resulting mixtures using polyacrylamide gels. Single bands

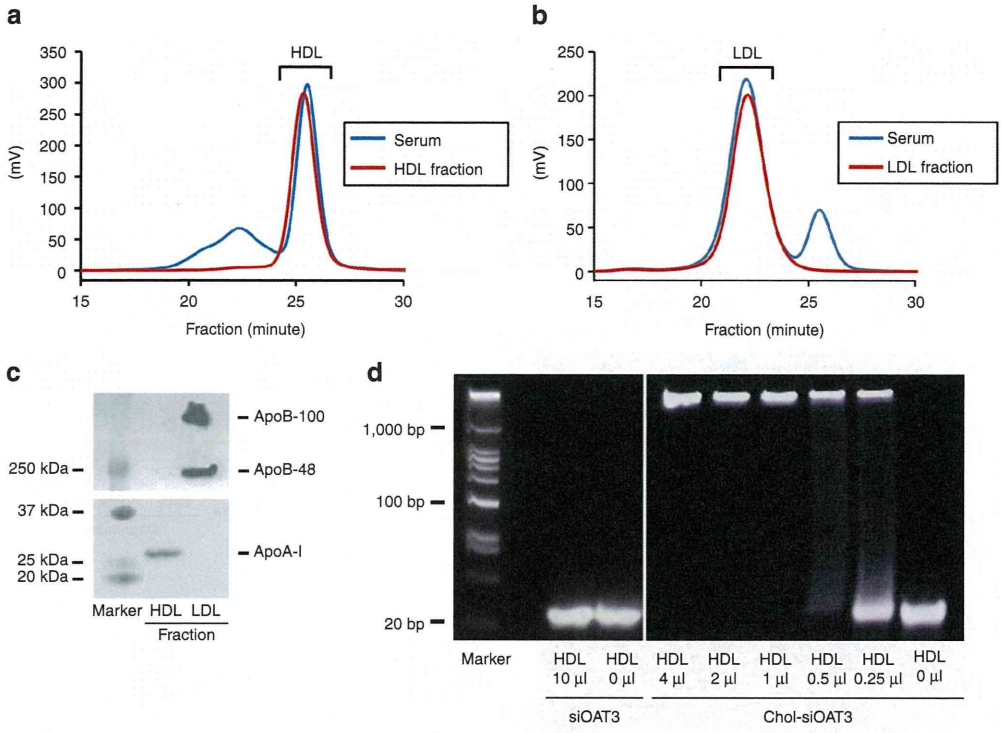

Figure 2 *Ex vivo* incorporation of Chol-siOAT3 into extracted endogenous lipoproteins. (**a**) HPLC analysis showing cholesterol levels of the serum and HDL fraction obtained from wild-type mice. (**b**) HPLC analysis showing cholesterol levels of the serum and LDL fraction obtained from LDL receptor-deficient (*LDLR*$^{-/-}$) mice. (**c**) Western blotting of ApoA-I and ApoB in the HDL and LDL fractions. (**d**) Gel-shift assay of siOAT3 and Chol-siOAT3. Electrophoretic mobility was examined using a 12% polyacrylamide gel after 100 pmol of each short-interfering RNA (siRNA) were incubated with different volumes of the HDL fraction. ApoA-I, apolipoprotein A-I; ApoB, apolipoprotein B; Chol-siOAT3, cholesterol-conjugated siRNA targeting *organic anion transporter 3* mRNA; HDL, high-density lipoprotein; HPLC, high-performance liquid chromatography; LDL, low-density lipoprotein; OAT3, organic anion transporter 3; siOAT3, unconjugated siRNA targeting *OAT3* mRNA.

were seen for siOAT3, both with and without the HDL fraction, at the position of ~21 nucleotides (**Figure 2d**). In contrast, mixtures of 100 pmol of Chol-siOAT3 and 1 µl and more of the HDL fraction did not show any bands corresponding to 21 nucleotides (**Figure 2d**). These mixtures were considered to be stable for at least 24 hours *in vivo* because the intensity and mobility of the mixtures did not change after the incubation with mouse sera at 37 °C for 24 hours (data not shown). Similar patterns of bands were seen when siOAT3 or Chol-siOAT3 was mixed with the LDL fraction (data not shown). Taken together, these results indicate that Chol-siOAT3 is incorporated into HDL and LDL in a saturable manner, whereas siOAT3 is not incorporated into these lipoproteins at all. We decided to mix 1 µl of the HDL or LDL fraction per 100 pmol of Chol-siOAT3 for animal experiments because Chol-siOAT3 could be fully incorporated into HDL or LDL at this ratio.

Delivery of Chol-siOAT3 into BCECs by intravenous injection

After siOAT3 and/or Chol-siOAT3 were injected into mice intravenously, we examined the extent of their delivery to the brain histologically. For this purpose, we utilized siRNAs labeled with Cy3 at the 5′-ends of the antisense strands. We injected 10 mg/kg of siOAT3 or Chol-siOAT3 alone [in phosphate-buffered saline (PBS)], or the same dosage of Chol-siOAT3 after its incorporation into HDL or LDL, into the tail vein. Brains of mice were taken 1 hour after the injection, and the frozen sections of the striatum were subjected to confocal laser imaging. We found no Cy3 signals in the brains after the injection of siOAT3 alone (**Figure 3a**). When mice were injected with Chol-siOAT3 without lipoproteins (Chol-siOAT3/PBS) or Chol-siOAT3 with the LDL fraction (Chol-siOAT3/LDL), there were faint Cy3 signals along the blood capillary vessels in the striatum (**Figure 3a**). In contrast, robust Cy3 signals were observed when mice were injected with Chol-siOAT3 with the HDL fraction (Chol-siOAT3/HDL) (**Figure 3a**). Similar findings were seen in all other areas of the brain, including the cerebral cortex, hippocampus, cerebellum, and the brainstem.

In mice injected with Chol-siOAT3/HDL, higher magnification of the brain sections revealed that Cy3 signals were located in the cytoplasm of BCECs that were marked immunologically by antibodies against von Willebrand factor (**Figure 3b**). There were no Cy3 signals in other cells of the brain, such as neurons or glia, indicating that Chol-siOAT3 could not pass through the BBB. Moreover, we found no Cy3 signals in the endothelial cells of the aorta and lung which were taken simultaneously at euthanization (data not shown).

For the detection of Chol-siOAT3 itself in the BCECs, we injected Chol-siOAT3 (10 mg/kg) with and without the lipoprotein fraction and performed northern blotting of small RNAs extracted from the small vascular fraction of the brain[21] 3 hours after injection with a probe corresponding to the antisense strand of Chol-siOAT3. The content of BCECs in the small vascular fraction of the brain was previously estimated to be ~50%[11] and thus,

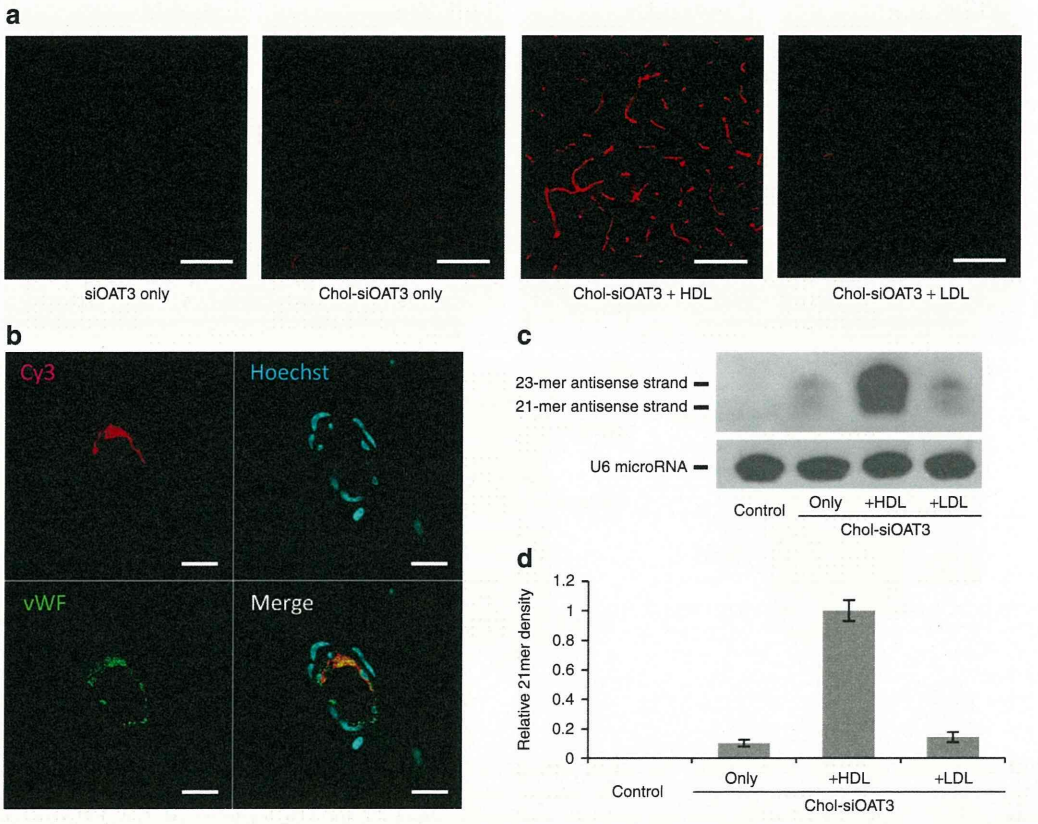

Figure 3 Delivery of Chol-siOAT3 into BCECs by intravenous injection. (**a**) Confocal laser images of frozen striatal sections prepared after intravenous injection of Cy3-labeled siOAT3 or Chol-siOAT3 (10 mg/kg), with and without the lipoprotein fraction. Bar = 100 µm. (**b**) Confocal laser images of frozen striatal sections prepared after intravenous injection of Cy3-labeled Chol-siOAT3 (10 mg/kg) along with HDL fraction. Sections were stained with Hoechst 33342 and immunolabeled with antibodies against vWF. Bar = 20 µm. (**c**) Northern blotting for the detection of antisense sequences of Chol-siOAT3 and the mouse U6 microRNA sequence in the small vascular fraction of the brain after injection of Chol-siOAT3 (10 mg/kg), with or without lipoprotein fractions. (**d**) The bars represent 21-mer band densities under the given conditions relative to band density of internal control, U6 microRNA. "Control" means uninjected; data are expressed as mean values ± SEM (n = 3). BCEC, brain capillary endothelial cell; Chol-siOAT3, cholesterol-conjugated short-interfering RNA targeting *organic anion transporter 3* mRNA; HDL, high-density lipoprotein; LDL, low-density lipoprotein; OAT3, organic anion transporter 3; siOAT3, unconjugated siRNA targeting *OAT3* mRNA; vWF, von Willebrand factor.

the detection of the antisense strand of Chol-siOAT3 by northern blotting was easier in this concentrated fraction than in the entire brain. The 21-mer band other than the 23-mer band was clearly detected when mice were injected with Chol-siOAT3/HDL (**Figure 3c**), suggesting that the 23-mer antisense strands had been cleaved by Dicer in the cytoplasm of BCECs. The density of the 21-mer band was much reduced when mice were injected with Chol-siOAT3/PBS or Chol-siOAT3/LDL (**Figure 3c,d**), demonstrating that the delivery of Chol-siOAT3 was only a little in these conditions. Taken together, these results indicate that Chol-siOAT3 is selectively delivered to the BCECs in the brain after intravenous injection and that the delivery is markedly enhanced when Chol-siOAT3 is incorporated into HDL before its injection into mice.

Gene silencing by intravenous injection of Chol-siOAT3 along with the HDL fraction

We assessed the extent of gene silencing after the intravenous injection of Chol-siOAT3. Mice were injected with 10 mg/kg Chol-siOAT3 with or without a lipoprotein fraction three times at 12-hour intervals, and were euthanized 6 hours after the last injection. Because OAT3 is exclusively expressed at endothelial cells in the brain, we could evaluate *OAT3* mRNA levels in BCECs by analyzing these levels in the entire brain. Quantitative reverse transcriptase-PCR (RT-PCR), which was performed using total RNA extracted from whole-brain homogenates, showed almost no reduction in *OAT3* mRNA levels when mice were injected with Chol-siOAT3/PBS or Chol-siOAT3/LDL (**Figure 4a**). In contrast, when mice were injected with Chol-siOAT3/HDL, *OAT3* mRNA levels in the brain were reduced by ~50% ($P < 0.01$; **Figure 4a**). We also evaluated *OAT3* mRNA levels in the kidneys of these mice because OAT3 was also expressed at the epithelial cells of the renal proximal tubules,[22] but there was no reduction (data not shown). The mRNA levels of interferon-β, interferon-γ, and tumor necrosis factor-α were not increased in the brains of these mice and there was no increase in the levels of interferon-α in the blood samples which were collected at euthanization from the mice injected with Chol-siOAT3/HDL, suggesting that there was no immune stimulatory effect contributing to the silencing activity (data not shown).

When mice were injected three times each with 1.0, 3.3, or 10 mg/kg of Chol-siOAT3 along with the HDL fraction (for total doses of 3, 10, and 30 mg/kg Chol-siOAT3), the 10 and 30 mg/kg total doses resulted in significant and dose-dependent reductions in *OAT3* mRNA levels (**Figure 4b**). We found no effects in

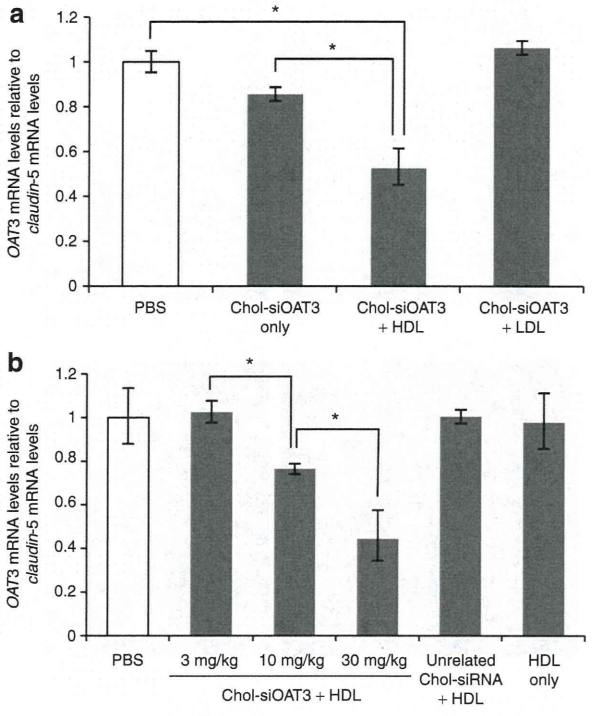

Figure 4 Gene silencing by intravenous injection of Chol-siOAT3 along with the HDL fraction. (**a**) Quantitative RT-PCR showing organic anion transporter 3 (*OAT3*) mRNA levels in whole-brain homogenates after the injection of Chol-siOAT3 (10 mg/kg), with and without lipoprotein fractions, three times at 12-hour intervals. The data shown are relative to claudin-5 mRNA levels and are expressed as mean values ± SEM ($n = 4$, $^*P < 0.01$). (**b**) Quantitative RT-PCR showing *OAT3* mRNA levels in whole-brain homogenates after the injection of different doses (1.0, 3.3, and 10 mg/kg) of Chol-siOAT3 with the HDL fraction, unrelated Chol-siRNA (10 mg/kg) with the HDL fraction, and HDL fraction only, three times at 12-hour intervals (Total injected dose is shown). The data shown are relative to claudin-5 mRNA levels and are expressed as mean values ± SEM ($n = 4$, $^*P < 0.01$). Chol-siOAT3, cholesterol-conjugated siRNA targeting *OAT3* mRNA; HDL, high-density lipoprotein; LDL, low-density lipoprotein; OAT3, organic anion transporter 3; PBS, phosphate-buffered saline; RT-PCR, reverse transcriptase-PCR.

the brain when mice were treated with an unrelated Chol-siRNA targeting *ApoB* mRNA (total dose 30 mg/kg) along with the HDL fraction, while there was a reduction of ~40% in the *ApoB* mRNA levels in the liver which was taken simultaneously at euthanization (data not shown). These results indicate that Chol-siOAT3 efficiently cleaves *OAT3* mRNA in BCECs when Chol-siOAT3 is incorporated into HDL before its injection into mice.

Receptor-mediated uptake of Chol-siOAT3/HDL into BCECs

We investigated the mechanism of delivery of Chol-siOAT3/HDL into BCECs. We thought that apolipoprotein E (ApoE) in HDL would most probably work as a ligand because of its important role in lipid transport.[23] First, we isolated endogenous HDL fractions from the sera of ApoE-deficient ($ApoE^{-/-}$ HDL)[24] and WT mice (WT HDL). To be able to make appropriate comparisons, we adjusted the mixed volume of each HDL fraction to have the same molecular amount of HDL-cholesterol. We then injected Cy3-labeled Chol-siOAT3 (10 mg/kg) into WT mice along with WT or $ApoE^{-/-}$ HDL fraction and compared the histological findings 1 hour later. The brain sections revealed similar Cy3 signals along the blood capillary vessels under both conditions (**Figure 5a**), suggesting that exogenous $ApoE^{-/-}$ HDL must recruit ApoE rapidly from the endogenous lipoproteins in the blood circulation of WT mice. Next, we injected the same dose of Cy3-labeled Chol-siOAT3 into $ApoE^{-/-}$ mice along with WT or $ApoE^{-/-}$ HDL fraction. Robust Cy3 signals were observed when Cy3-labeled Chol-siOAT3 was injected along with WT HDL fraction (**Figure 5b**), indicating that the receptors for HDL were intact in the BCECs of $ApoE^{-/-}$ mice. In contrast, there were remarkably reduced Cy3 signals when Cy3-labeled Chol-siOAT3 was injected into $ApoE^{-/-}$ mice along with $ApoE^{-/-}$ HDL fraction (**Figure 5b**), demonstrating that the delivery of Chol-siOAT3/HDL was mainly ApoE-dependent.

We tried further to identify the putative receptor for Chol-siOAT3/HDL in BCECs. Among several lipoprotein receptors expressed in BCECs, we hypothesized that LDLR was most likely to be responsible for the uptake of Chol-siOAT3/HDL because of its notably high affinity for ApoE.[23,25] The brain sections of $LDLR^{-/-}$ mice injected with Cy3-labeled Chol-siOAT3 along with WT HDL fraction revealed remarkably reduced Cy3 signals compared to the brain sections of WT mice injected with the same solution (**Figure 5c**), suggesting that Chol-siOAT3/HDL was taken up into BCECs mainly via LDLR.

Moreover, we assessed the gene silencing effect in the brains of $ApoE^{-/-}$ and $LDLR^{-/-}$ mice. $ApoE^{-/-}$ mice were injected with 10 mg/kg Chol-siOAT3 with $ApoE^{-/-}$ HDL and $LDLR^{-/-}$ mice were injected with 10 mg/kg Chol-siOAT3 with WT HDL three times at 12-hour intervals, and were euthanized 6 hours after the last injection. Quantitative RT-PCR showed no reduction in *OAT3* mRNA levels in the brains of $ApoE^{-/-}$ and $LDLR^{-/-}$ mice (**Figure 5d**). Taken together, these results indicate that the uptake of Chol-siOAT3/HDL into BCECs was mainly mediated by ApoE and LDLR in mice.

In vitro examinations of receptor-mediated uptake

We assessed *in vitro* whether LDLR could actually mediate the uptake of endogenous HDL. For this purpose, we utilized HEK293T cells transfected with a LDLR-expressing plasmid or a mock plasmid. The HDL fraction extracted from the sera of WT mice was mixed with a fluorescent lipid probe of BODIPY and was incubated in the culture medium of the HEK293T cells for 3 hours. LDLR-overexpressing cells showed marked BODIPY signals in the cytoplasm, whereas the cells transfected with mock plasmid showed almost no signals (**Figure 6a**), suggesting that extracted endogenous HDL could be taken up via LDLR.

Moreover, we evaluated *in vitro* whether the uptake of Chol-siOAT3/HDL into BCECs was mediated by scavenger receptor class B type I (SRBI) because SRBI was known as a major HDL receptor in the liver and was reported to be also expressed at BCECs.[26] For this purpose, we utilized the culture cells of conditionally immortalized brain capillary endothelium of mice origin, TM-BBB,[27] in which we confirmed the expression of *SRBI* mRNA by RT-PCR (data not shown). The cells were treated with a SRBI inhibitor, BLT-1,[28] and then incubated with 1 μmol/l of Cy3-labeled Chol-siOAT3/HDL for 30 minutes. Cy3 signals in the cytoplasm of TM-BBB cells were not decreased by BLT-1 (**Figure 6b**),

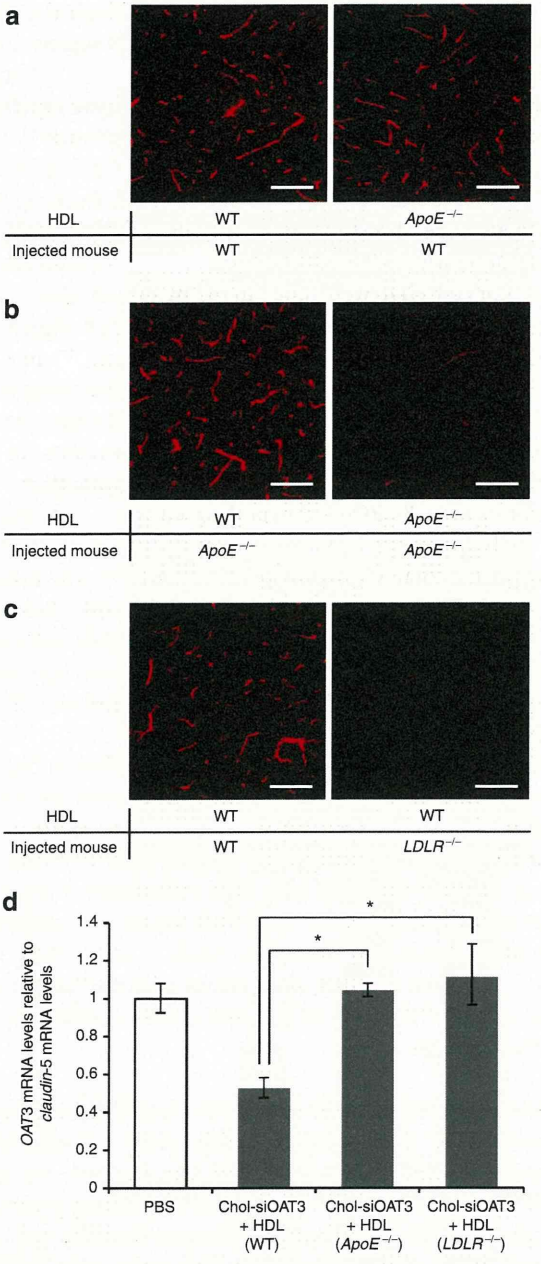

Figure 5 Receptor-mediated uptake of Chol-siOAT3/HDL into BCECs. (**a**) Confocal laser images of frozen striatal sections of WT mice after the injection of Cy3-labeled Chol-siOAT3 (10 mg/kg) with the HDL fraction extracted from the sera of WT or ApoE-deficient (*ApoE*$^{-/-}$) mice. Bar = 100 µm. (**b**) Confocal laser images of frozen striatal sections of *ApoE*$^{-/-}$ mice after the injection of Cy3-labeled Chol-siOAT3 (10 mg/kg) with the HDL fraction extracted from the sera of WT or *ApoE*$^{-/-}$ mice. Bar = 100 µm. (**c**) Confocal laser images of frozen striatal sections of WT and *LDLR*$^{-/-}$ mice after the injection of Cy3-labeled Chol-siOAT3 (10 mg/kg) with the HDL fraction extracted from the sera of WT mice. Bar = 100 µm. (**d**) Quantitative RT-PCR showing organic anion transporter 3 (*OAT3*) mRNA levels in whole-brain homogenates of WT, *ApoE*$^{-/-}$, and *LDLR*$^{-/-}$ mice after the injection of Chol-siOAT3 (10 mg/kg) with the HDL fraction, three times at 12-hour intervals. WT and *LDLR*$^{-/-}$ mice were injected with WT HDL, and *ApoE*$^{-/-}$ mice were injected with *ApoE*$^{-/-}$ HDL. The data shown are relative to claudin-5 mRNA levels and are expressed as mean values ± SEM ($n = 4$, *$P < 0.01$). ApoE, apolipoprotein E; BCEC, brain capillary endothelial cell; Chol-siOAT3, cholesterol-conjugated siRNA targeting *OAT3* mRNA; HDL, high-density lipoprotein; LDLR, low-density lipoprotein receptor; OAT3, organic anion transporter 3; WT, wild-type.

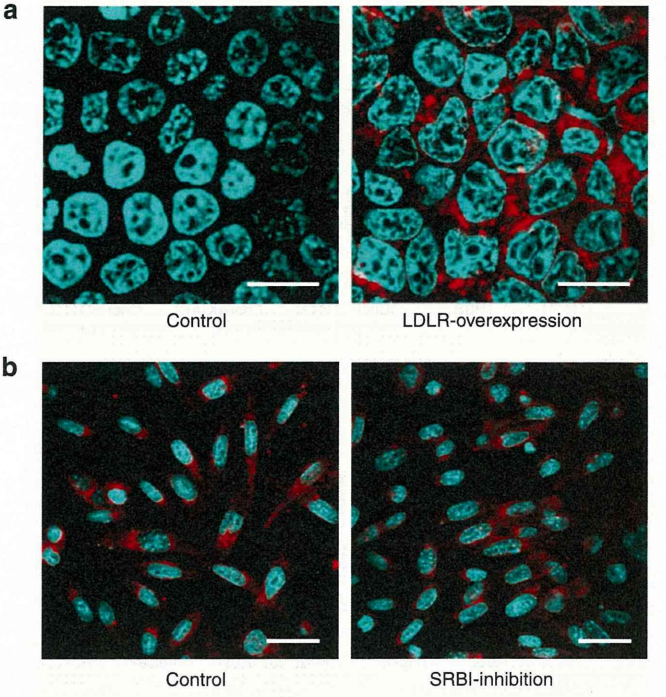

Figure 6 *In vitro* examinations of receptor-mediated uptake. (**a**) Confocal laser images of HEK293T cells transfected with a mock plasmid (Control) or a LDLR-expressing plasmid (LDLR-overexpression) 3 hours after incubation in the culture medium containing BODIPY-labeled HDL (red). Cells were stained with Hoechst 33342. Bar = 20 µm. (**b**) Confocal laser images of TM-BBB cells incubated with 1 µmol/l of Cy3-labeled Chol-siOAT3/HDL for 30 minutes with and without a pretreatment by 1 µmol/l of SRBI inhibitor. "Control" means no pretreatment by SRBI inhibitor. Cells were stained with Hoechst 33342. Bar = 20 µm. Chol-siOAT3, cholesterol-conjugated siRNA targeting *OAT3* mRNA; HDL, high-density lipoprotein; LDLR, low-density lipoprotein receptor; OAT3, organic anion transporter 3; SRBI, scavenger receptor class B type I.

suggesting that SR-BI was not a major receptor responsible for the uptake of Chol-siOAT3/HDL into BCECs.

DISCUSSION

In this study, we achieved efficient delivery of siRNA into BCECs by utilizing endogenous lipoproteins. We showed that Chol-siOAT3 was efficiently delivered into BCECs when incorporated into HDL before its intravenous injection, and that the mechanism of delivery was mainly receptor-mediated uptake.

When Chol-siOAT3 was injected without any lipoproteins, the delivery into BCECs was quite limited and resulted in very little gene silencing. Two explanations may account for this result. First, Chol-siOAT3 not incorporated into lipoproteins is rapidly removed from blood circulation through filtration in the kidneys and by uptake into the reticuloendothelial system such as the spleen, lymph nodes, and bone marrow.[10] Second, Chol-siOAT3 probably forms aggregates with other serum proteins, especially albumin,[15] resulting in its decreased incorporation into endogenous, circulating HDL. Chol-siOAT3 may attach itself to the plasma membrane of BCECs by virtue of its lipophilicity, but it is unlikely to be taken up by a nonspecific fluid-phase mechanism because there is minimal pinocytosis in BCECs.[1]

BCECs express lipoprotein receptors such as the LDLR, SRBI, and LDLR-related proteins.[2,26,29] The interaction of lipoproteins and BCECs has been investigated mostly from the perspective of lipoprotein transport to the brain across the BBB, rather than into the BCECs themselves. Plasma LDL can bind to LDLR in BCECs and pass through them via transcytosis to supply lipids to the brain.[29,30] Moreover, it has been suggested that plasma HDL can transport α-tocopherol to the brain by binding to SRBI and move via transcytosis across the BCECs.[26] Serum lipoproteins must also get transported into the BCECs themselves, especially for supplying cholesterol, because an earlier study using primary cultures of microvascular endothelial cells have shown that cholesterol synthesis in these cells decreases after addition of lipoproteins to the medium.[31] However, the precise mechanism of this transport—which lipoproteins are taken up into the BCECs and which receptors are responsible for this *in vivo* uptake—has not been elucidated.

Our results indicate that HDL works as an efficient vector for transporting Chol-siOAT3 into the BCECs, being mainly mediated by ApoE as the ligand and LDLR as the receptor. LDL binds to LDLR with ApoB-100 as a ligand, whereas HDL is also bound tightly to LDLR with ApoE as a ligand.[32,33] Investigations using human fibroblasts demonstrated that ApoE is necessary for HDL to not only bind to LDLR, but also to be internalized into the cells.[33] In the examinations using LDLR-overexpressing cells, we have also demonstrated that LDLR can mediate the uptake of endogenous HDL. On the other hand, SRBI was not considered to be a major receptor responsible for the uptake of Chol-siOAT3/HDL into BCECs because SRBI-inhibitor did not prevent the uptake of Chol-siOAT3/HDL into TM-BBB cells. SRBI is essentially responsible for the reverse cholesterol transport into hepatocytes and is mainly associated with the collection of cholesterol from the vascular endothelial cells into HDL, not the supply of cholesterol from HDL to these cells.[34] Therefore, we think it reasonable that the contribution of SRBI to the uptake of Chol-siOAT3/HDL into BCECs might be small. We suppose that in addition to LDLR, LDLR-related proteins can possibly mediate this uptake because LDLR-related proteins may be responsible for the supply of cholesterol into BCECs by virtue of its high affinity for ApoE.

Here we can ask why the delivery of Chol-siOAT3/LDL to BCECs via LDLR was not sufficiently achieved in WT mice, in spite of LDL uptake being the main function of LDLR. One possible explanation is the unique lipoprotein profile in rodents, which is different from those seen in other species. Because the rate of hepatic LDL clearance in rodents is 40 times greater than that in humans,[35] Chol-siOAT3/LDL may be getting rapidly eliminated from the blood circulation into the liver, resulting in limited distribution to other tissues or organs in mice. This explanation is consistent with the findings of an earlier study showing that Chol-siRNA was delivered almost exclusively to the mouse liver when it was incorporated into LDL, whereas with HDL, it was also distributed to the kidney, adrenal gland, ovary, stomach, and intestine.[15] Our negative result of *OAT3* mRNA suppression in the kidneys by Chol-siOAT3/HDL is probably and simply because the epithelial cells of the renal proximal tubules, in which OAT3 is expressed, are lined by the basement membrane and therefore do not directly face the blood circulation. As another explanation of the insufficient delivery of Chol-siOAT3/LDL to BCECs, we cannot rule out the possibility that LDL in $LDLR^{-/-}$ mice may have some unknown property that may be causing low affinity for LDLR. As a therapeutic approach in humans, LDL as well as HDL has a potential to work as another effective vector of Chol-siRNA to deliver the siRNA to BCECs in humans.

Our strategy of siRNA delivery using an HDL vector accomplished a 50–60% reduction in the target mRNA levels in BCECs. Depending on the target molecules, even this partial gene silencing effect can be expected to achieve a sufficient therapeutic outcome. A promising candidate gene for the treatment of AD is RAGE, which facilitates the transport of Aβ across the BBB into the brain[8] and therefore introduces the associated oxidative stress and neuroinflammation that characterize the disease.[9] The levels of RAGE are reported to be ~2.5-fold higher in the brains of AD patients than in age-matched controls.[8] Moreover, it is demonstrated that the inhibition of RAGE in BCECs could alleviate AD pathology in a transgenic AD mouse model in which the level of RAGE was approximately twice in the cerebral cortex of transgenic AD mice when compared with their nontransgenic littermate controls.[9] Thus, even a 50–60% reduction in the levels of RAGE in BCECs could be beneficial as a therapeutic intervention for AD patients.

The practicality of our strategy using endogenous lipoprotein should be also discussed. The volume of the HDL and LDL fraction in our experiments was half of mouse serum, and from a single series of ultracentrifugations, we obtained these fractions for 25 injections when mixed with 10 mg/kg of Chol-siRNA. We needed just one mouse for obtaining the HDL fraction for three injections with 10 mg/kg of Chol-siRNA, which accomplished a 50–60% reduction of target mRNA levels in BCECs. The dosing volume of 10 ml/kg body weight in our experiments is generally employed in the actual intravenous administration of blood products to patients, suggesting the feasibility of our strategy in the clinical situations.

Because lipoprotein vectors have been reported to accumulate mainly in the liver,[15] an enhancing their tropism toward BCECs would help to decrease the dose of Chol-siRNA and the lipoprotein vector. A recent study accomplished the delivery of increased amounts of a gene to BCECs by inserting polypeptides, selected from a phage library by *in vivo* panning, into the binding site of the adeno-associated virus vector to its receptor.[36] Similar approaches of engineering with polypeptides for Chol-siRNA and lipoprotein vectors should facilitate their enhanced targeting to BCECs and result in greater efficiency in gene silencing.

As another possible improvement of our strategy, recombinant lipoproteins can be better siRNA vectors because of their purity and homogeneity. Concerning the ApoE-based delivery, synthetic carriers including micelles and liposomes have been actually utilized for the delivery to BCECs *in vitro*.[37,38] However, it is not certain that recombinant lipoproteins can incorporate Chol-siRNA in the same manner as endogenous lipoprotein and that these artificial lipoproteins can be efficiently delivered to BCECs by the same receptor-mediated mechanism *in vivo*.

In summary, this is the first report to demonstrate the concept of an endogenous lipoprotein vector for the efficient delivery of siRNA into BCECs in mice via an intravenous injection. This concept of siRNA delivery can be advanced as a promising clinical

strategy for gene silencing to treat various diseases involving BCECs.

MATERIALS AND METHODS

siRNAs. All siRNAs were chemically synthesized at Hokkaido System Science (Sapporo, Japan). Cholesterol-conjugated siRNA targeting *OAT3* mRNA (Chol-siOAT3) was constituted from the corresponding sense strand: 5′-CCA UUA UCU UGA AUG UGG AAU*-cholesterol-3′ and antisense strand: 5′-AUU CCA CAU UCA AGA UAA UGg* u*G-3′. The lower case letters represent 2′-*O*-methyl sugar modification and the asterisks represent phosphorothioate linkages. Unconjugated siRNA targeting *OAT3* mRNA (siOAT3) was composed of the sense strand: 5′-CCA UUA UCU UGA AUG UGG AA*U-3′ and the same antisense strand as Chol-siOAT3. The unrelated siRNAs prepared for *in vitro* mRNA targeting were as follows: mouse claudin-5 (sense strand: 5′-CGU UGG AAA UUC UGG GUC UUU-3′, antisense strand: 5′-AGA CCC AGA AUU UCC AAC GUU-3′); mouse superoxide dismutase-1 (sense strand: 5′-GGU GGA AAU GAA GAA AGU ACA AAG ACU-3′, antisense strand: 5′-AGU CUU UGU ACU UUC UUC AUU UCC ACC UU-3′); and cholesterol-conjugated siRNA for *in vitro* and *in vivo* targeting of apolipoprotein-B mRNA (sense strand: 5′-GUC AUC ACA CUG AAU ACC AAU*-cholesterol-3′, antisense strand: 5′-AUU GGU AUU CAG UGU GAU GAc* a*C-3′).

Cholesterol was covalently conjugated via a cholesteryl-triethyleneglycol phosphoramidite linker (10-1975; Glen Research, Sterling, VA). For histological examinations, the 5′-ends of the antisense strands of siOAT3 and Chol-siOAT3 were labeled with Cy3. For the generation of siRNA duplexes, equimolar amounts of sense and antisense strands were heated in PBS at 95 °C for 5 minutes and slowly cooled to room temperature.

In vitro gene silencing. Mouse *OAT3* cDNA was subcloned from pGEM-HEN/Roct (OAT3) into the *Renilla* luciferase expression vector, psi-CHECK-1 (Promega, Fitchburg, WI). Neuro2a cells were transfected with 20 ng of a *Renilla* luciferase-fused *OAT3* expression vector, 50 ng of a firefly luciferase expression vector, pGL3 (Promega), and siRNA at different concentrations in each well of 24-well plates. Changes in *Renilla* luciferase activity were normalized to firefly luciferase activity. The luciferase activities were analyzed 24 hours after transfection by using the Dual Luciferase System (Promega).

Animals. Female WT imprinting control region mice (Oriental Yeast, Tokyo, Japan) were used to evaluate the extent of delivery of Chol-siOAT3 with and without lipoprotein fractions. Investigations of the mechanism of delivery of Chol-siOAT3/HDL were conducted in female $LDLR^{-/-}$ and $ApoE^{-/-}$ mice on a C57BL/6J background (The Jackson Laboratory, Bar Harbor, ME) and also with female WT C57BL/6J mice (Oriental Yeast). Mice were 8–10 weeks of age at the time of the studies and were kept on a 12-hour light/dark cycle in a pathogen-free animal facility with free access to food and water. All animal experiments were performed in accordance with the Ethical and Safety Guidelines for Animal Experiments of the Tokyo Medical and Dental University.

Isolation of lipoproteins. Lipoproteins were isolated from the sera of WT, $LDLR^{-/-}$, and $ApoE^{-/-}$ mice by ultracentrifugation, according to a modification of a method described earlier.[39] First, a half volume of a solution of density 1.006 g/ml was layered onto one volume of mouse serum and centrifuged for 2.4 hours at 337,000*g* at 16 °C. Second, one volume of the lower solution was mixed with a half volume of a solution of density 1.182 g/ml and centrifuged for 3.6 hours at 337,000*g* at 16 °C. The half volume of the upper solution was set aside for use in experiments as the LDL fraction, and one volume of the lower solution was mixed with a half volume of a solution of density 1.478 g/ml and centrifuged for 7.5 hours at 266,000*g* at 16 °C. The half volume of the upper solution obtained after this third centrifugation contained HDL and was used in experiments as the HDL fraction.

Western blotting analysis. Two microliters of HDL or LDL fraction were collected in 18 μl of homogenate buffer [20 mmol/l Tris–HCl (pH 7.4), 0.1% SDS, 0.1% Triton X-100, 0.01% sodium deoxycholate, and 1× complete protease inhibitor cocktail [Roche Diagnostics, Mannheim, Germany)]. The total protein mixture was separated by electrophoresis in a 5–20% polyacrylamide gel (ATTO, Tokyo, Japan) and transferred onto polyvinylidene difluoride membranes. Blots were probed with a goat antibody against ApoA-I (1:500, sc-23605; Santa Cruz Biotechnology, Santa Cruz, CA) and ApoB (1:500, sc-11795; Santa Cruz Biotechnology), and then incubated with an anti-goat secondary antibody (1:2,000, sc-2020; Santa Cruz Biotechnology) tagged with horseradish peroxidase. Blots were visualized with the aid of SuperSignal West Femto Maximum Sensitivity Substrate (Thermo Fisher Scientific, Waltham, MA) and analyzed with a ChemiDoc System (Bio-Rad, Hercules, CA).

Gel-shift assay. One hundred pmol of siOAT3 and Chol-siOAT3 were added to 0–10 μl of the HDL or LDL fraction. The samples were resolved by electrophoresis in a 12% polyacrylamide gel for 1 hour at 100 V. Two micrograms of siRNA ladder marker (Takara Bio, Otsu, Japan) was used as a size standard for siRNA. The siRNAs were visualized under ultraviolet light after staining the gel with ethidium bromide in Tris-borate-EDTA buffer.

Injection of siRNAs. Each siRNA was injected slowly into the tail veins of mice at a dosing volume of 10 ml/kg body weight in a single dose of 10 mg/kg for histological examinations and northern blotting analyses, and was injected three times in doses of 1.0, 3.3, or 10 mg/kg body weight at 12-hour intervals for quantitative RT-PCR.

Histological examination. Brains of mice were fixed in 4% paraformaldehyde/PBS for 12 hours. The fixed specimens were snap-frozen in liquid nitrogen and brain sections of 16-μm thickness were prepared by using a LEICA CM3050 S cryostat (Leica Microsystems, Wetzlar, Germany). The sections were stained with Hoechst 33342 (Sigma-Aldrich, St Louis, MO) to visualize the nuclei and were immunolabeled with antibodies against von Willebrand factor (1:100, A0082; Dako, Glostrup, Denmark) to visualize vascular endothelial cells. This was followed by incubation with a fluorescein isothiocyanate-conjugated secondary antibody (1:50, AP106F; Millipore, Billerica, MA). All images were acquired with an LSM 510 confocal laser scanning microscope (Carl Zeiss MicroImaging, Göttingen, Germany).

Small vascular fractionation of the brain and northern blotting analysis. The small vascular fraction of the brain was prepared according to a modification of a method reported earlier.[21] Briefly, brains of mice were homogenized in PBS and centrifuged for 5 minutes at 800*g*. The pellet was suspended in a 15% dextran solution and centrifuged for 10 minutes at 4,500*g* at 4 °C. The pellet was resuspended in 5 mmol/l PBS and, after incubation for 10 minutes, was centrifuged for 5 minutes at 800*g*. Small RNAs containing fewer than 200 nucleotides were extracted from the above final pellet of small vessels using MirVana (Ambion, Austin, TX). The RNA was condensed with Ethachinmate (Nippon Gene, Tokyo, Japan) and 1.2 μg of the RNA was separated by electrophoresis in a 14% polyacrylamide-urea gel and transferred to a Hybond-N^+ membrane (Amersham Biosciences, Piscataway, NJ). The blot was hybridized with a probe corresponding to the siRNA antisense sequence or with the mouse U6 microRNA sequence (as an internal control) which had been labeled with fluorescein using a Gene Images 3′-Oligolabelling Kit (Amersham Biosciences). The signals were visualized by Gene Images CDP-star Detection Kit (Amersham Biosciences).

Quantitative RT-PCR assay. Total RNA was extracted from whole-brain homogenates with Isogen (Nippon Gene). DNase-treated RNA (2.5 μg) was reverse-transcribed with Super Script III and Random Hexamers (Life Technologies, Carlsbad, CA). The cDNAs were amplified by

the quantitative TaqMan system by using the Light Cycler 480 Real-Time PCR Instrument (Roche Diagnostics). The primers and probes for mouse *OAT3* (Mm00459534_m1), claudin-5 (Mm00727012_s1), interferon-β (Mm00439546_s1), interferon-γ (Mm00801778_m1), and tumor necrosis factor-α (Mm00443258_m1) were designed by Life Technologies. Relative *OAT3* mRNA levels were calculated in comparison to claudin-5 mRNA levels, which were used as a BCEC-specific internal control.

Interferon-α analysis. The levels of interferon-α in the blood samples were analyzed by mouse interferon-α ELISA Kit (PBL Biomedical Laboratories, Piscataway, NJ) according to the manufacturers' protocol.

In vitro examinations of receptor-mediated uptake. Mouse serum HDL was labeled with BODIPY by a mixture of the HDL fraction and the solution of cholesteryl BODIPY 542/563 C11 (Life Technologies). HEK293T cells were grown in poly-D-lysine 4-well culture slides (BD, Franklin Lakes, NJ) and were transfected with 600 ng of mouse LDLR-expressing plasmid (Origene, Rockville, MD) or the same dose of mock plasmid by using Lipofectamine 2000 (Life Technologies). Twenty four hours after the transfection of the plasmids, the mixed solution containing 11 μl of the HDL fraction was added to 400 μl of the culture medium. After incubation for 3 hours, the cells were stained with Hoechst 33342 (Sigma-Aldrich) and were fixed in 4% paraformaldehyde/PBS.

TM-BBB cells (generously provided by Tetsuya Terasaki, PhD, Graduate School of Pharmaceutical Sciences, Tohoku University) were grown in collagen-I 4-well culture slides (BD) at 33 °C. The cells were treated with 1 μmol/l of SRBI inhibitor, BLT-1 (373210; Merck, Darmstadt, Germany) for 1 hour and then, were incubated with 1 μmol/l of Cy3-labeled Chol-siOAT3/HDL. After incubation for 30 minutes, the cells were stained with Hoechst 33342 (Sigma-Aldrich) and were fixed in 4% paraformaldehyde/PBS.

All images were acquired with an LSM 510 confocal laser scanning microscope (Carl Zeiss MicroImaging).

Statistical analysis. All data represent means ± SEM. Student's *t*-test was used to determine the significance of differences between two groups in quantitative RT-PCR assays.

ACKNOWLEDGMENTS

The authors thank Sumio Ohtsuki, PhD, Graduate School of Pharmaceutical Sciences, Tohoku University, for his helpful advice, and Mizuko Osaka, PhD, Department of Life Science and Medical Ethics, Graduate School, Tokyo Medical and Dental University, for her technical support. This work was supported by grants from the Ministry of Health, Labour, and Welfare of Japan (#2212070 and #2212148) and a grant from the Ministry of Education, Science and Culture of Japan (#20659138). This work was done in Tokyo, Japan. The authors declared no conflict of interest.

REFERENCES

1. Pardridge, WM (2007). Blood-brain barrier genomics. *Stroke* **38**(2 Suppl): 686–690.
2. Abbott, NJ, Patabendige, AA, Dolman, DE, Yusof, SR and Begley, DJ (2010). Structure and function of the blood-brain barrier. *Neurobiol Dis* **37**: 13–25.
3. Zlokovic, BV (2008). The blood-brain barrier in health and chronic neurodegenerative disorders. *Neuron* **57**: 178–201.
4. Frijns, CJ and Kappelle, LJ (2002). Inflammatory cell adhesion molecules in ischemic cerebrovascular disease. *Stroke* **33**: 2115–2122.
5. Danton, GH and Dietrich, WD (2003). Inflammatory mechanisms after ischemia and stroke. *J Neuropathol Exp Neurol* **62**: 127–136.
6. Correale, J and Villa, A (2007). The blood-brain-barrier in multiple sclerosis: functional roles and therapeutic targeting. *Autoimmunity* **40**: 148–160.
7. Simka, M (2009). Blood brain barrier compromise with endothelial inflammation may lead to autoimmune loss of myelin during multiple sclerosis. *Curr Neurovasc Res* **6**: 132–139.
8. Yan SD, Chen X, Fu J, Chen M, Zhu H, Roher A *et al.* (1996). RAGE and amyloid-beta peptide neurotoxicity in Alzheimer's disease. *Nature* **382**: 685–691.
9. Deane, R, Du Yan, S, Submamaryan, RK, LaRue, B, Jovanovic, S, Hogg, E *et al.* (2003). RAGE mediates amyloid-beta peptide transport across the blood-brain barrier and accumulation in brain. *Nat Med* **9**: 907–913.
10. Whitehead, KA, Langer, R and Anderson, DG (2009). Knocking down barriers: advances in siRNA delivery. *Nat Rev Drug Discov* **8**: 129–138.
11. Hino, T, Yokota, T, Ito, S, Nishina, K, Kang, YS, Mori, S *et al.* (2006). *In vivo* delivery of small interfering RNA targeting brain capillary endothelial cells. *Biochem Biophys Res Commun* **340**: 263–267.
12. Campbell, M, Kiang, AS, Kenna, PF, Kerskens, C, Blau, C, O'Dwyer, L *et al.* (2008). RNAi-mediated reversible opening of the blood-brain barrier. *J Gene Med* **10**: 930–947.
13. Fuest, C, Bankstahl, M, Winter, P, Helm, M, Pekcec, A and Potschka, H (2009). *In vivo* down-regulation of mouse brain capillary P-glycoprotein: a preliminary investigation. *Neurosci Lett* **464**: 47–51.
14. Pfrieger, FW (2003). Cholesterol homeostasis and function in neurons of the central nervous system. *Cell Mol Life Sci* **60**: 1158–1171.
15. Wolfrum, C, Shi, S, Jayaprakash, KN, Jayaraman, M, Wang, G, Pandey, RK *et al.* (2007). Mechanisms and optimization of *in vivo* delivery of lipophilic siRNAs. *Nat Biotechnol* **25**: 1149–1157.
16. Sano, M, Sierant, M, Miyagishi, M, Nakanishi, M, Takagi, Y and Sutou, S (2008). Effect of asymmetric terminal structures of short RNA duplexes on the RNA interference activity and strand selection. *Nucleic Acids Res* **36**: 5812–5821.
17. Ohtsuki, S, Asaba, H, Takanaga, H, Deguchi, T, Hosoya, K, Otagiri, M *et al.* (2002). Role of blood-brain barrier organic anion transporter 3 (OAT3) in the efflux of indoxyl sulfate, a uremic toxin: its involvement in neurotransmitter metabolite clearance from the brain. *J Neurochem* **83**: 57–66.
18. Soutschek, J, Akinc, A, Bramlage, B, Charisse, K, Constien, R, Donoghue, M *et al.* (2004). Therapeutic silencing of an endogenous gene by systemic administration of modified siRNAs. *Nature* **432**: 173–178.
19. Ishibashi, S, Brown, MS, Goldstein, JL, Gerard, RD, Hammer, RE and Herz, J (1993). Hypercholesterolemia in low density lipoprotein receptor knockout mice and its reversal by adenovirus-mediated gene delivery. *J Clin Invest* **92**: 883–893.
20. Usui, S, Hara, Y, Hosaki, S and Okazaki, M (2002). A new on-line dual enzymatic method for simultaneous quantification of cholesterol and triglycerides in lipoproteins by HPLC. *J Lipid Res* **43**: 805–814.
21. Kanda, T, Yoshino, H, Ariga, T, Yamawaki, M and Yu, RK (1994). Glycosphingolipid antigens in cultured bovine brain microvascular endothelial cells: sulfoglucuronosyl paragloboside as a target of monoclonal IgM in demyelinative neuropathy [corrected]. *J Cell Biol* **126**: 235–246.
22. Rizwan, AN and Burckhardt, G (2007). Organic anion transporters of the SLC22 family: biopharmaceutical, physiological, and pathological roles. *Pharm Res* **24**: 450–470.
23. Mahley, RW (1988). Apolipoprotein E: cholesterol transport protein with expanding role in cell biology. *Science* **240**: 622–630.
24. Zhang, SH, Reddick, RL, Piedrahita, JA and Maeda, N (1992). Spontaneous hypercholesterolemia and arterial lesions in mice lacking apolipoprotein E. *Science* **258**: 468–471.
25. Hatters, DM, Peters-Libeu, CA and Weisgraber, KH (2006). Apolipoprotein E structure: insights into function. *Trends Biochem Sci* **31**: 445–454.
26. Balazs, Z, Panzenboeck, U, Hammer, A, Sovic, A, Quehenberger, O, Malle, E *et al.* (2004). Uptake and transport of high-density lipoprotein (HDL) and HDL-associated alpha-tocopherol by an *in vitro* blood-brain barrier model. *J Neurochem* **89**: 939–950.
27. Hosoya, K, Tetsuka, K, Nagase, K, Tomi, M, Saeki, S, Ohtsuki, S *et al.* (2000). Conditionally immortalized brain capillary endothelial cell lines established from a transgenic mouse harboring temperature-sensitive simian virus 40 large T-antigen gene. *AAPS PharmSci* **2**: E27.
28. Nieland, TJ, Shaw, JT, Jaipuri, FA, Duffner, JL, Koehler, AN, Banakos, S *et al.* (2008). Identification of the molecular target of small molecule inhibitors of HDL receptor SR-BI activity. *Biochemistry* **47**: 460–472.
29. Goti, D, Balazs, Z, Panzenboeck, U, Hrzenjak, A, Reicher, H, Wagner, E *et al.* (2002). Effects of lipoprotein lipase on uptake and transcytosis of low density lipoprotein (LDL) and LDL-associated alpha-tocopherol in a porcine *in vitro* blood-brain barrier model. *J Biol Chem* **277**: 28537–28544.
30. Dehouck, B, Fenart, L, Dehouck, MP, Pierce, A, Torpier, G and Cecchelli, R (1997). A new function for the LDL receptor: transcytosis of LDL across the blood-brain barrier. *J Cell Biol* **138**: 877–889.
31. Roux, FS, Mokni, R, Hughes, CC, Clouet, PM, Lefauconnier, JM and Bourre, JM (1989). Lipid synthesis by rat brain microvessel endothelial cells in tissue culture. *J Neuropathol Exp Neurol* **48**: 437–447.
32. Jeon, H and Blacklow, SC (2005). Structure and physiologic function of the low-density lipoprotein receptor. *Annu Rev Biochem* **74**: 535–562.
33. Mahley, RW and Innerarity, TL (1977). Interaction of canine and swine lipoproteins with the low density lipoprotein receptor of fibroblasts as correlated with heparin/manganese precipitability. *J Biol Chem* **252**: 3980–3986.
34. Connelly, MA and Williams, DL (2004). Scavenger receptor BI: a scavenger receptor with a mission to transport high density lipoprotein lipids. *Curr Opin Lipidol* **15**: 287–295.
35. Dietschy, JM and Turley, SD (2002). Control of cholesterol turnover in the mouse. *J Biol Chem* **277**: 3801–3804.
36. Chen, YH, Chang, M and Davidson, BL (2009). Molecular signatures of disease brain endothelia provide new sites for CNS-directed enzyme therapy. *Nat Med* **15**: 1215–1218.
37. Sauer, I, Dunay, IR, Weisgraber, K, Bienert, M and Dathe, M (2005). An apolipoprotein E-derived peptide mediates uptake of sterically stabilized liposomes into brain capillary endothelial cells. *Biochemistry* **44**: 2021–2029.
38. Leupold, E, Nikolenko, H and Dathe, M (2009). Apolipoprotein E peptide-modified colloidal carriers: the design determines the mechanism of uptake in vascular endothelial cells. *Biochim Biophys Acta* **1788**: 442–449.
39. Hatch, FT (1968). Practical methods for plasma lipoprotein analysis. *Adv Lipid Res* **6**: 1–68.

HUMAN GENE THERAPY 22:711–719 (June 2011)

DOI: 10.1089/hum.2010.083

High-Density Lipoprotein Facilitates *In Vivo* Delivery of α-Tocopherol–Conjugated Short-Interfering RNA to the Brain

Yoshitaka Uno,[1] Wenying Piao,[1] Kanjiro Miyata,[2] Kazutaka Nishina,[1] Hidehiro Mizusawa,[1] and Takanori Yokota[1]

Abstract

We originally reported the use of vitamin E (α-tocopherol) as an *in vivo* vector of short-interfering RNA (siRNA) to the liver. Here, we apply our strategy to the brain. By combining high-density lipoprotein (HDL) as a second carrier with α-tocopherol–conjugated siRNA (Toc-siRNA) in the brain, we achieved dramatic improvement of siRNA delivery to neurons. After direct intracerebroventricular (ICV) infusion of Toc-siRNA/HDL for 7 days, extensive and specific knock-down of a target gene, β-site amyloid precursor protein cleaving enzyme 1 (*BACE1*), was observed in both mRNA and protein levels, especially in the cerebral cortex and hippocampus. This new delivery method achieved a much more prominent down-regulation effect than conventional silencing methods of the brain gene, i.e., ICV infusion of nonconjugated siRNA or oligonucleotides. With only 3 nmol Toc-siRNA with HDL, BACE1 mRNA in the parietal cortex could be reduced by ~70%. We suppose that this dramatic improvement of siRNA delivery to the brain is due to the use of lipoprotein receptor–mediated endocytosis because the silencing efficiency was significantly increased by binding of Toc-siRNA to the lipoprotein, and in contrast, was clearly decreased in lipoprotein-receptor knockout mice. These results suggest exogenous siRNA could be used clinically for otherwise incurable neurological diseases.

Introduction

THE POSSIBLE THERAPEUTIC APPLICATIONS of short-interfering RNA (siRNA) cover a wide spectrum of disorders, including cancer, infectious diseases, and inherited diseases. There has been much interest in the clinical applications of siRNA to neurological diseases such as Alzheimer's disease (AD), Huntington's disease, Parkinson's disease, and amyotrophic lateral sclerosis. However, delivery of siRNA to the brain has not been well established.

For *in vivo* delivery of siRNA, viral vectors and high-pressure, high-volume intravenous injection methods have been described. However, these approaches have limitations in clinical practice due to their side effects. Much progress has been reported on intravenous administration of siRNA to the liver using cationic liposomes, nanoparticles, and cell-penetrating peptides (Zimmermann *et al.*, 2006; Moschos *et al.*, 2007; Rozema *et al.*, 2007; Wolfrum *et al.*, 2007; Akinc *et al.*, 2008, 2009; Gao *et al.*, 2009). Ligand conjugation for receptor-mediated uptake system is also expected to be another possible delivery method *in vivo* (Kumar *et al.*, 2007).

We recently published a report of efficient systemic delivery of siRNA to the liver by using conjugation with α-tocopherol (Nishina *et al.*, 2008). We expected that the most effective *in vivo* carrier would be a molecule that is essential for target tissue cells but cannot be synthesized within the cells. Vitamins fit these requirements well, and the least toxic vitamin, even at high doses, is vitamin E (Kappus and Diplock, 1992). α-Tocopherol is a lipophilic natural molecule and has physiological pathways from blood to the brain as well as to the liver. Orally ingested α-tocopherol is absorbed at the ileum, incorporated into chylomicrons, and transferred to very-low-density lipoprotein (VLDL) in the liver by α-tocopherol transfer protein (αTTP). VLDL containing α-tocopherol is metabolized to low-density lipoprotein (LDL) and HDL, which supply α-tocopherol to all tissue cells via their respective lipoprotein receptors (Rigotti, 2007). The delivery pathway of α-tocopherol to the brain has not been

[1]Department of Neurology and Neurological Science, Graduate School, Tokyo Medical and Dental University, Bunkyo-ku, Tokyo 113-0034, Japan.
[2]Division of Clinical Biotechnology, Center for Disease Biology and Integrative Medicine, Graduate School of Medicine, The University of Tokyo, Bunkyo-ku, Tokyo 113-0034, Japan.

well investigated. Brain endothelial cells have a receptor-mediated uptake system of α-tocopherol from α-tocopherol–containing HDL and LDL through each receptor (Goti *et al.*, 2002; Mardones *et al.*, 2002; Qian *et al.*, 2005). After α-tocopherol enters the brain, αTTP may have an important role in supplying α-tocopherol to neurons and glial cells. We and others showed that α-tocopherol in the brain was almost depleted in $\alpha TTP^{-/-}$ mice and was markedly decreased even in $\alpha TTP^{-/-}$ mice fed an α-tocopherol–rich diet resulting in increased serum α-tocopherol (Yokota *et al.*, 2001; Gohil *et al.*, 2008). αTTP is expressed in astrocytes (Hosomi *et al.*, 1998), and cholesterol, as a major lipid, is transferred to neurons and glial cells from astrocytes by HDL-like particles synthesized in astrocytes (Pfrieger, 2003; Vance *et al.*, 2005; Herz and Chen, 2006). We postulated that α-tocopherol could be delivered to neurons and glial cells by HDL-like particles in the brain. Although serum HDL and brain HDL-like particles are different in their composition and origin, their size and density are similar and both supply lipids through lipoprotein receptors with ApoE as a ligand (Vance *et al.*, 2005). Therefore, we attempted to use serum HDL as a carrier vector for α-tocopherol–conjugated siRNA to neurons and glial cells with delivery by direct ICV infusion.

Materials and Methods

siRNAs

α-Tocopherol–conjugated and Cy3-labeled siRNAs were synthesized by Hokkaido System Science (Sapporo, Japan). The sequences for the sense and antisense strands of siBACE are as follows: siBACE sense, 5′-GAAcCuAuGCGAuGCGA AuGUUUAU*A*C-3′; antisense, 5′-guauaaACAUuCGCAuC GCAUAgGUuC*U*U-3′. 2′-*O*-methyl–modified nucleotides are in lower case, and phosphorothioate linkages are represented by asterisks. α-Tocopherol and Cy3 fluorophore were covalently bound to the 5′-end of antisense and sense strands, respectively. siRNA duplexes were generated by annealing equimolar amounts of complementary sense and antisense strands.

In vitro *siRNA transfection assay*

Neuro2a cells were transfected with each siRNA at 10 n*M* with Lipofectamine RNAiMAX, as described by the vendor (Invitrogen, Carlsbad, CA). For quantitative real-time polymerase chain reaction (qRT-PCR), total RNA was extracted and 2 μg of RNA was reverse-transcribed with Superscript III kit (Invitrogen). qRT-PCR was performed using the LightCycler 480 Probes Master and LightCycler 480 II (Roche Diagnostics, Mannheim, Germany) according to the manufacturer's instructions. Primers for mouse BACE1 and glyceraldehyde-3-phosphate dehydrogenase (GAPDH) mRNAs were designed by Applied Biosystems (Foster City, CA).

For Western blot analysis, transfected cells were harvested 48 hr post transfection. Cell pellets were purified for cytosolic fraction with NE-PER nuclear and cytoplasmic extraction reagents (Thermo Fisher Scientific, Waltham, MA). Samples were separated by 10% denaturing polyacrylamide gel electrophoresis (PAGE) and transferred onto polyvinylidene difluoride membranes. Blots were probed with a rabbit antibody against BACE1 (1:500, AB5832; Millipore, Billerica, MA) and confirmed with a mouse antibody against β-tubulin (1:2000, MAB1637; Chemicon, Temecula, CA). Blots were incubated with anti-rabbit or anti-mouse secondary antibodies (1:1000) tagged with horseradish peroxidase. Blots were visualized with SuperSignal West Femto Maximum Sensitivity Substrate (Thermo Fisher Scientific) and analyzed by a ChemiDoc system (Bio-Rad, Hercules, CA).

HDL collection

The HDL fraction was prepared with sequential ultracentrifugation by a method described previously (Hatch and Lees, 1968). In brief, one volume of mouse serum and a half volume of density 1.182 solution was mixed and centrifuged for 3.5 hr at 450,000 × *g* at 16°C. A half volume of density 1.478 solution was then added to one volume of the bottom layer. The tubes were mixed and centrifuged for 4 hr, 50 min at 450,000 × *g* at 16°C. The top fraction containing HDL was used in the experiments.

HDL labeling with dipyrromethene boron difluoride

To prepare dipyrromethene boron difluoride (BODIPY) working solution, cholesteryl BODIPY 542/563 C11 powder (Invitrogen) was dissolved in dimethyl sulfoxide at a concentration of 0.5 μg/ml. The BODIPY working solution and HDL fraction were mixed at a volume ratio of 1:5 and vortexed before use.

In vitro *LDL receptor overexpression study*

HEK293T cells were grown in four-chamber slides (1×10^5 cells/well) and transfected using Lipofectamine 2000 (Invitrogen) according to the manufacturer's protocol. Briefly, 600 ng of mouse LDL receptor (LDLR; cDNA clone MGC:62289) expressing plasmid (Origene, Rockville, MD) and 60 ng pEGFP (Clontech, Mountain View, CA) or reporter plasmid alone were mixed with 1 μl of Lipofectamine 2000 and added to each well. Following 24 hr of incubation, wells were gently washed three times with Dulbecco's modified Eagle medium (DMEM), then BODIPY-labeled HDL containing DMEM (1:30 volume ratio) was added to each well and the cells were further incubated for 3 hr. After incubation, cells were fixed with 4% paraformaldehyde and nuclei were counterstained with 4′,6-diamidino-2-phenylindole.

For Western blot analysis, cells were harvested 24 hr post transfection. Cells were lysed in homogenate buffer (20 m*M* Tris-HCl [pH 7.4], 0.1% SDS, 0.1% Triton X-100, 0.01% sodium deoxycholate, 1×Complete protease inhibitor cocktail [Roche Diagnostics]). Five micrograms of total protein was separated by 10% PAGE, and the proteins were transferred onto membranes and immunoblotted as described. Blots were probed with a rabbit antibody against LDLR (1:1000; Novus Biologicals, Littleton, CO) and confirmed with a mouse antibody against GAPDH (1:3000; Chemicon).

Fluorescence correlation spectroscopy analysis

To control the total fluorescent signal under saturation, the final concentration of Toc-siRNA-Cy3 or siRNA-Cy3 was fixed at 50 n*M* and varying concentrations of unlabeled Toc-siRNA or unlabeled siRNA respectively (0 to 75 μ*M*) were added to 10-μl aliquots of the HDL fraction. Measurements were performed using the ConfoCor 3 module in combination with a LSM 510 laser scanning microscope (Carl Zeiss

MicroImaging GmbH, Göttingen, Germany) equipped with the C-Apochromat 40×/1.2W objective. A HeNe laser (543 nm) was used for Cy3-labeled siRNA excitation and emission was filtered through a 560- to 615-nm band pass filter. Samples were placed into an eight-well Lab-Tek chambered coverglass (Nalge Nunc International, Rochester, NY) and measured at room temperature. Autocorrelation curves obtained from 10 measurements with a sampling time of 20 sec were fitted with the ConfoCor 3 software package to determine diffusion time of samples.

Animals and human cerebrospinal fluid

Female Crlj:CD1 (ICR) mice aged 3 to 4 months old (27 to 30 g; Oriental Yeast, Tokyo, Japan) were used for ICV infusion experiments. For $LDLR^{-/-}$ mice, B6.129S7-Ldlr (tm1Her)/J (Jackson Laboratory, Bar Harbor, ME) and wild-type (WT) C57BL/6J (Oriental Yeast) were used. Cerebrospinal fluid was collected from a healthy human volunteer. All procedures used in animal studies and the use of human samples were approved by the ethical committee of Tokyo Medical and Dental University and were consistent with local and state regulations as applicable.

ICV infusion

Mice were anesthetized with isoflurane (1.5% to 2.0%). Osmotic minipumps (model 1007D; Alzet, Cupertino, CA) were filled with phosphate-buffered saline (PBS) or free Toc-siBACE or Toc-siBACE/HDL and connected with Brain Infusion Kit 3 (Alzet). A brain-infusion cannula was placed −0.5 mm posterior to the bregma at midline for infusion into the dorsal third ventricle (Thakker *et al.*, 2004).

Confocal immunofluorescense and histochemical microscopy analyses

The fixed brains were sectioned at 10 μm with a cryostat (Leica, Wetzlar, Germany). For confocal immunofluorescense observation, sections were immunolabeled with antibodies against MAP2 (1:200, AB5622; Chemicon) and glial fibrillary acidic protein (GFAP, 1:500, G3893; Sigma, St. Louis, MO) followed by incubation with fluorescein isothiocyanate (FITC)-conjugated secondary antibodies. Images were obtained with LSM 510 META (Zeiss). Obtained images were transmitted to image analysis software (WinROOF, Mitani, Tokyo, Japan) and analyzed to estimate the areas of each color. To examine regional BACE1 protein expression, sections were immunolabeled with a mouse monoclonal antibody (1:50, MAB5308; Chemicon) in combination with M.O.M. immunodetection kit (Vector Laboratories, Burlingame, CA) and developed with 3,3′-diaminobenzidine (DAB).

In vivo *analyses for siRNA activity*

Fresh frozen brain samples were sectioned at 10 μm and transferred onto a membrane slide (Leica), fixed, and dehydrated through a serial gradient of ethanol, 95%, 75%, 50%, 50%, 75%, 95%, 100%, for 30 sec each and once in 100% ethanol for 2 min followed by xylene for 5 min. Sample slides were set on fluorescence equipped laser microdissection system (AS LMD, Leica), and regions of interest were cut at a fixed square measure from three sections (hippocampal formation, 8.4×10^6 μm^2; parietal cortex, 5.1×10^6 μm^2). For qRT-PCR assays, total cellular RNA was extracted (PicoPure RNA isolation kit; Arcturus, Sunnyvale, CA) and total RNA was reverse-transcribed. qRT-PCR was performed as described for the *in vitro* siRNA transfection assay. For Western blots, cut samples were directly collected in 25 μl of homogenate buffer. Total proteins were separated by 10% PAGE, transferred onto membranes, and immunoblotted as described. For Northern blots, block brain samples, approximately 50 mg each, were homogenized and purified for small RNAs by MirVana (Ambion, Austin, TX). Small RNA samples were loaded 20 μg for each, separated by 24% denaturing PAGE,

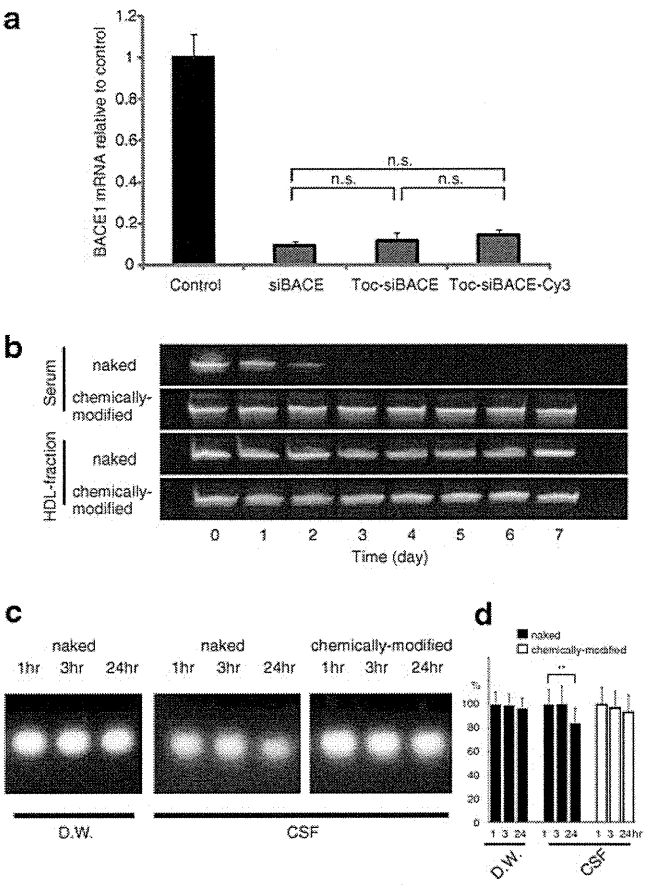

FIG. 1. *In vitro* validation of RNAi activity and stability for modified siRNAs against BACE1. **(a)** RNAi activity in mouse Neuro2a cells was measured by transfecting nonconjugated siBACE, Toc-siBACE, and Toc-siBACE-Cy3. Quantitative reverse-transcription polymerase chain reaction (qRT-PCR) analysis of BACE1 mRNA levels showed efficient target silencing after tocopherol conjugation and Cy3 labeling. (Data are shown as mean values ± SEM, $n = 3$. One-way ANOVA followed by Tukey-Kramer multiple comparisons, n.s.; not significant). **(b)** Naked siRNA or chemically modified siRNA was incubated with mouse serum or high-density lipoprotein (HDL) fraction at 37°C for up to 7 days. Samples were separated by nondenaturing 18% PAGE. **(c)** Chemically modified siRNA and naked siRNA were incubated in distilled water (D.W.) or cerebrospinal fluid (CSF) at 37°C up to 24 hr. Samples were separated on nondenaturing 2% agarose. **(d)** Densitometric analysis of the band intensities showed substantial degradation of naked siRNA in CSF. Error bars (SD) are derived from triplicates. $^{**}p < 0.01$, Student's t test.

transferred to nylon membrane (Hybond-N+, Amersham, Piscataway, NJ), and then hybridized with DNA probes labeled by DIG oligonucleotide 3′ end labeling kit (GE Healthcare, Piscataway, NJ). Signals were developed with CDP-Star (GE Healthcare).

Results

In vitro *validation of efficiency and stability of Toc-siRNA*

Using Neuro2a cells, we checked RNA interference (RNAi) activity of eight different siRNAs targeting BACE1 mRNA (NM_011792) (siBACE), two from preceding reports (Kao *et al.*, 2004; Singer *et al.*, 2005) and six newly designed sequences, and selected the best siBACE (siBACE-8) (Supplementary Fig. S1a; Supplementary data are available online at www.liebertonline.com/hum). This siBACE was confirmed to suppress endogenous BACE1 protein as well (Supplementary Fig. S1b, c).

α-Tocopherol was covalently bound to the 5′ end of the antisense strand of the siRNA. According to previously reported principles (Nishina *et al.*, 2008), we made chemical modifications with phosphorothioate backbone linkage and sugar 2′-*O*-methylation on both sense and antisense strands for increasing stability of siRNA against endogenous ribonucleases. Furthermore, 5′ end of sense strand was labeled with Cy3 fluorophore to examine histological distribution of Toc-siRNA *in vivo*.

To confirm the influence of α-tocopherol conjugation and Cy3 labeling on RNAi activity, nonconjugated siBACE, Toc-siBACE, and Cy3-labeled Toc-siBACE (Toc-siBACE-Cy3) were transfected to Neuro2a cells at 10 n*M*. These modifications did not influence silencing activity of siBACE (Fig. 1a).

To check the stability of Toc-siBACE against ribonucleases, Toc-siBACE was incubated at 37°C with mouse serum, the HDL fraction of mouse serum, or human CSF. Naked siRNA was completely degraded in serum after incubation for 3 days. Chemically modified siRNA did not degrade for up to 7 days in serum, showing satisfactory protection against ribonucleases. Naked siRNA as well as chemically modified siRNA did not degrade in the HDL fraction after 7 days, suggesting that serum ribonucleases were eliminated after sequential ultracentrifugation (Fig. 1b). With a view to direct central administration, we also checked siRNA stability in CSF. Chemically modified siRNA did not degrade in CSF (Fig. 1c). Naked siRNA showed substantial degradation in CSF after 24 hr by densitometric analysis (Fig. 1d).

Toc-siRNA binding assay with HDL

For simplicity, Toc-siRNA-Cy3 is referred to hereafter as Toc-siRNA. To demonstrate the binding of Toc-siRNA and HDL, we conducted a gel-shift assay for evaluating interaction between these two molecules.

Nonconjugated siRNA incubated with the HDL fraction migrated almost identically to that incubated with PBS. Toc-siRNA incubated with the HDL fraction showed much lower mobility than that with PBS, indicating that the interaction of Toc-siRNA with HDL was due to lipophilic binding by the tocopherol moiety of Toc-siRNA (Fig. 2a). The ratio of

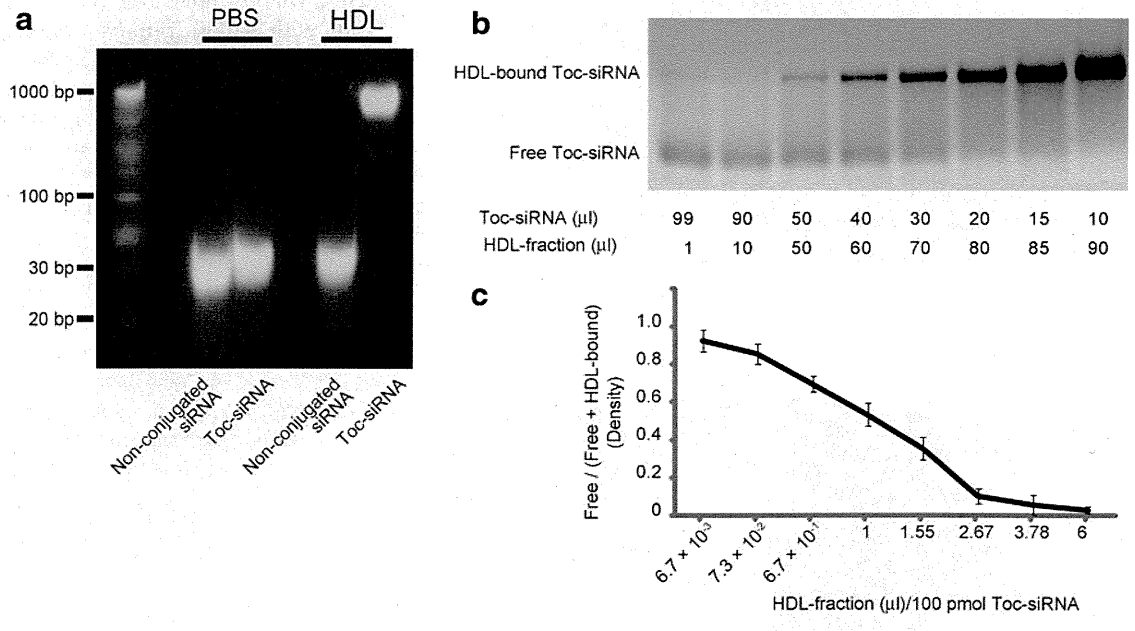

FIG. 2. Binding assay for Toc-siRNA and HDL. **(a)** 100 pmol nonconjugated siRNA or Toc-siRNA was added to 10 μl of phosphate-buffered saline (PBS) or the HDL fraction, and then samples were incubated at 37°C for 30 min. When incubated with PBS, Toc-siRNA showed slightly smaller mobility than nonconjugated siRNA on nondenaturing 2% agarose. It was assumed that the size and net charge of the molecule affected the migration change. When incubated with the HDL fraction, Toc-siRNA showed much smaller mobility than that with PBS, indicating the binding between Toc-siRNA and HDL. **(b)** Extensive gel-shift assay for Toc-siRNA and HDL binding. Varying volume ratios of 150 μM Toc-siRNA to HDL fraction were mixed and incubated at 37°C for 10 min. For a gel-shift assay, the loaded amount of Toc-siRNA was equivalent (100 pmol) for each lane and samples were separated on 2% agarose. **(c)** Densitometric analysis of free and HDL-bound Toc-siRNA. The *x*-axis shows the corresponding HDL-fraction volume in **b**. Error bars (SD) are derived from triplicates.

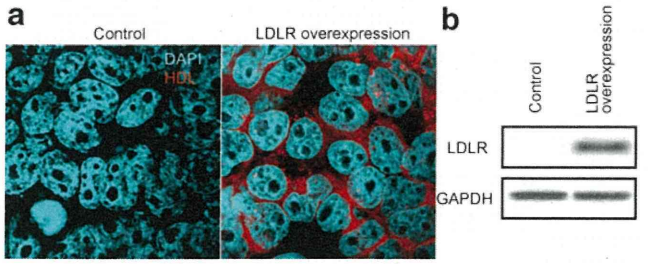

FIG. 3. Overexpression of low-density lipoprotein receptor (LDLR) facilitated HDL uptake *in vitro*. Wild-type (WT) and LDLR-overexpressed HEK293T cells were incubated with fluoro-labeled HDL (red signal). **(a)** LDLR-overexpressed cells showed intense signals of labeled HDL with dot-like cytosolic accumulation. **(b)** Western blots of HEK293T cells lysates for LDLR and GAPDH as a loading control.

Toc-siRNA to HDL fraction was determined by an extensive gel-shift assay and optical density measurements with varying ratios of Toc-siRNA to HDL fraction (Fig. 2b and c). The ratio was set at 20 μl of 150 μM Toc-siRNA to 80 μl of HDL fraction, where free Toc-siRNA almost disappeared. The binding of almost all the Toc-siRNA to HDL was also confirmed by fluorescence correlation spectroscopy analysis (Supplementary Fig. S2).

HDL uptake via LDLR in vitro

We hypothesized that serum HDL can be taken up by neurons and glial cells via LDLR because serum HDL has characteristics similar to HDL-like particles of the central nervous system (CNS) in its size, density, and apolipoproteins. To confirm this, we carried out an LDLR overexpression study *in vitro* by transfecting mouse LDLR-expressing plasmid to HEK293T cells. LDLR expression was confirmed by Western blot analysis (Fig. 3b). The mouse serum HDL fraction was labeled with fluorophore (BODIPY 542/563 C11) and applied to culture medium. LDLR-overexpressed cells showed marked HDL uptake, whereas mock-plasmid–transfected HEK293T cells as a negative control showed almost no HDL uptake (Fig. 3a).

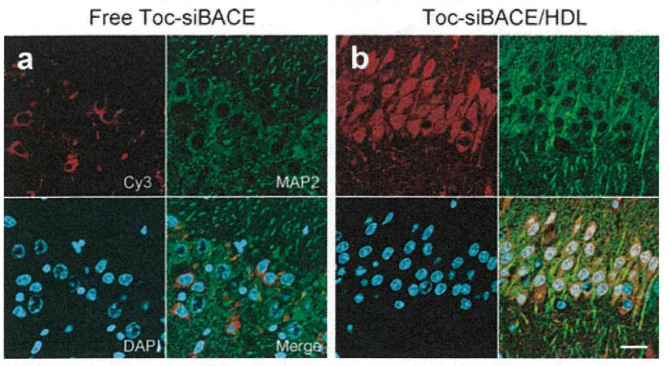

FIG. 4. Laser confocal microscopic images of MAP2-labeled hippocampus CA3 neurons infused with either **(a)** free Toc-siBACE or **(b)** Toc-siBACE/HDL. Nuclei were counterstained with 4′,6-diamidino-2-phenylindole (DAPI). Scale bar, 20 μm.

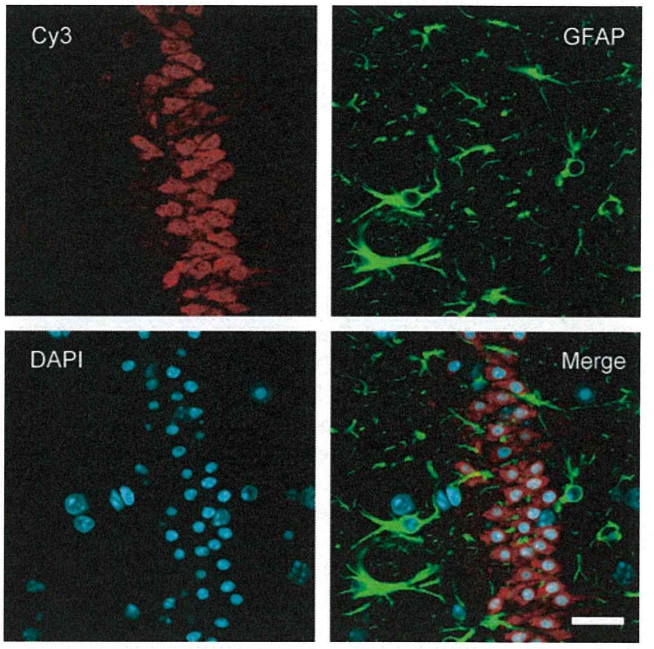

FIG. 5. Laser confocal microscopic observation for glial cell uptake of Toc-siBACE in the hippocampus CA3 region of a mouse infused with Toc-siBACE/HDL. Glial cells were detected by anti-GFAP antibody. Nuclei were counterstained with DAPI. Scale bar, 20 μm.

HDL enhanced in vivo *delivery of Toc-siRNA*

To test the performance of Toc-siRNA/HDL *in vivo*, Toc-siBACE bound to HDL was administered to the mouse brain by direct ICV infusion with osmotic pumps. Continuous ICV infusion of Toc-siBACE/HDL for 7 days achieved broader and more intense transduction of Toc-siBACE to the brain (Fig. 4b) than that of free Toc-siBACE (Fig. 4a), whereas ICV infusion of nonconjugated siBACE showed almost no signal in the brain (Supplementary Fig. S3).

The transduction of Toc-siBACE/HDL distributed broadly within the brain in the posterior frontal, parietal, and temporal areas and the hippocampal formation, and especially in areas more proximal to the lateral and third ventricles. In particular, intense signals were observed in the hippocampal neuronal cell layers and periventricular white matter.

By immunofluorescence microscopic observation, siRNA-transduced cells were mainly neuronal cells detected by anti-MAP2 antibody and showed an intense and homogenous Cy3 signal, rather than tiny dots, in the cytosol and often in the nucleus as well with Toc-siBACE/HDL–infused brain (Fig. 4b). Weaker cytosolic signal was also seen with free Toc-siBACE–infused brain (Fig. 4a). GFAP staining also depicted neuronal rather than glial uptake of Toc-siBACE in the cerebral cortex and hippocampus with Toc-siBACE/HDL–infused brain (Fig. 5).

In vivo *analyses of RNAi activity in the brain*

To measure the target mRNA reduction in the area where Toc-siRNA was transduced, we used laser dissection microscopy equipped with fluorescent observation system to capture Cy3 signal–positive regions directly. Free Toc-siBACE

could not elicit evident target gene silencing, whereas laser-dissected samples from Toc-siBACE/HDL–infused brain revealed significant reduction of target BACE1 mRNA at the hippocampal formation and parietal cortex (Fig. 6a; free Toc-siBACE vs. Toc-siBACE/HDL, hippocampus; 6% vs. 36%, parietal cortex; 13% vs. 64%, relative to control). Furthermore, neither free nontargeting Toc-siRNA (Toc-siApoB) nor Toc-siApoB/HDL affected target BACE1 mRNA level, indicating sequence specific cleavage.

Moreover, we could detect more prominent band of Dicer-cleaved antisense strand than that of the original antisense strand from Toc-siBACE/HDL–infused brain on siRNA Northern blot (Fig. 6b), indicating efficient delivery of Toc-siBACE to cytosol and its Dicer recognition.

Western blot analysis of BACE1 from signal positive regions in the parietal cortex of Toc-siBACE/HDL–infused brain showed substantial reduction of BACE1 protein (Fig. 6c and d; β-tubulin as a loading control, 52% reduction to control).

Regional repression of BACE1 protein was also evident by immunohistological examination. We could detect reduced DAB staining in the cerebral cortex, and the hippocampus, where siRNA transduction was confirmed under fluorescence microscopy (Fig. 7). Histological examination by hematoxylin-eosin (HE) staining of the Toc-siBACE/HDL–infused brain showed no obvious abnormality including cellular infiltration (Supplementary Fig. S4).

The uptake of Toc-siRNA/HDL was mediated by LDLR

Glial cells excrete ApoE-containing lipoprotein (HDL-like particles), and neurons incorporate the lipoprotein via receptor-mediated endocytosis. Several members of LDL receptor family (LDLR, low-density lipoprotein receptor-related protein 1 [LRP1], VLDL receptor [VLDLR]) are expressed in neurons and glial cells (Fan *et al.*, 2001). Amongst these receptors, LDLR is a cardinal one for metabolism of HDL-like particles (Vance *et al.*, 2005). We used $LDLR^{-/-}$ mice to see whether Toc-siRNA/HDL uptake is mediated by this receptor. $LDLR^{-/-}$ mice infused with Toc-siBACE/HDL showed much less Cy3 signals in the hippocampal neuronal cell layers than WT mice (Fig. 8a). In the periventricular

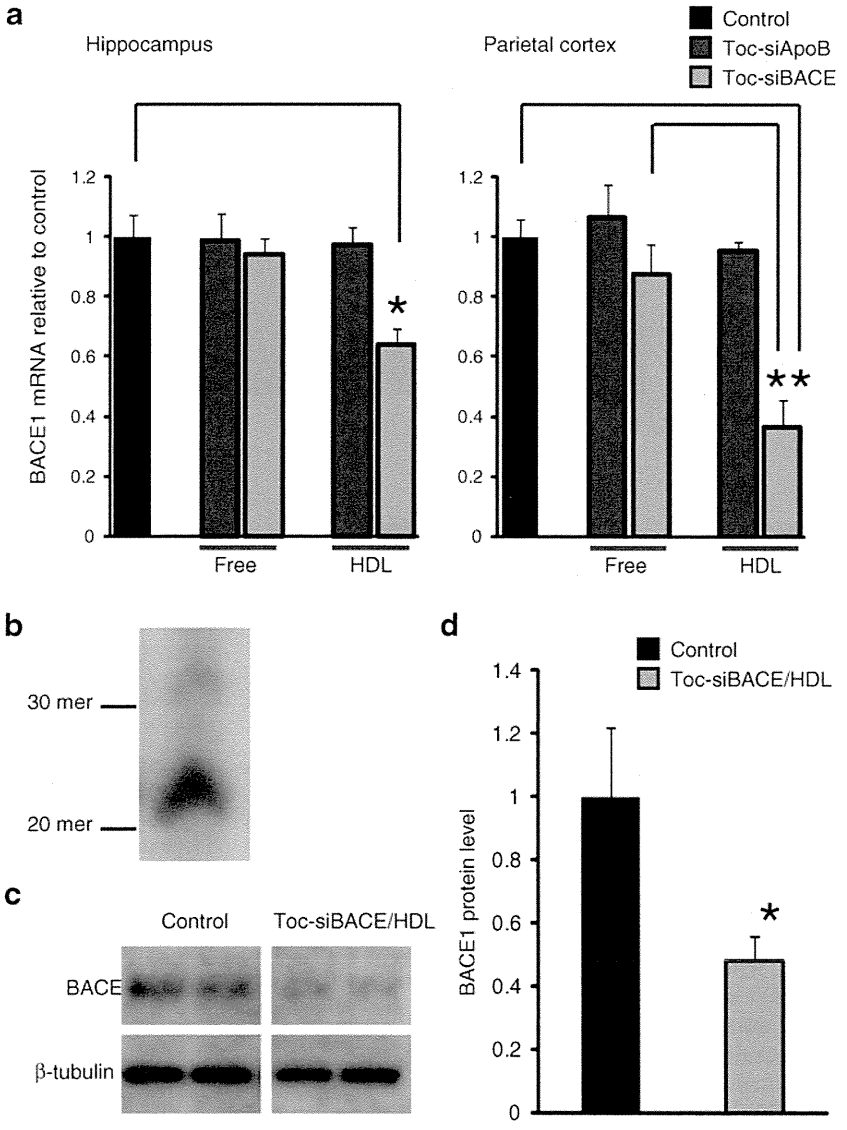

FIG. 6. *In vivo* analyses of RNAi activity of free Toc-siBACE and Toc-siBACE/HDL. **(a)** For qRT-PCR analyses, mRNA was purified from laser-dissected samples of the same square measure from each brain region of control brains (PBS infusion), free Toc-siRNA–infused or Toc-siRNA/HDL–infused brains. (Data are shown as mean values ± SEM, $n = 3$. One-way ANOVA followed by Tukey-Kramer multiple comparisons, $^{*}p < 0.05$, $^{**}p < 0.01$). **(b)** Northern blot analysis for Toc-siBACE. Small RNAs were purified from total homogenate of a 3-mm-thick brain section adjacent to the infusion site of the brain. Membrane was proved with the DIG-labeled DNA oligonucleotides of the sense strand. **(c)** For Western blot, total lysates of laser dissected samples of the same square measure from the parietal cortex region were immunoblotted with anti-BACE1 antibody and confirmed with anti-β-tubulin antibody as a loading control. **(d)** Bar graph shows BACE1/tubulin ratios from densitometry of bands in **c**. Values represent mean ± SEM. $^{*}p = 0.092$, Student's *t* test.

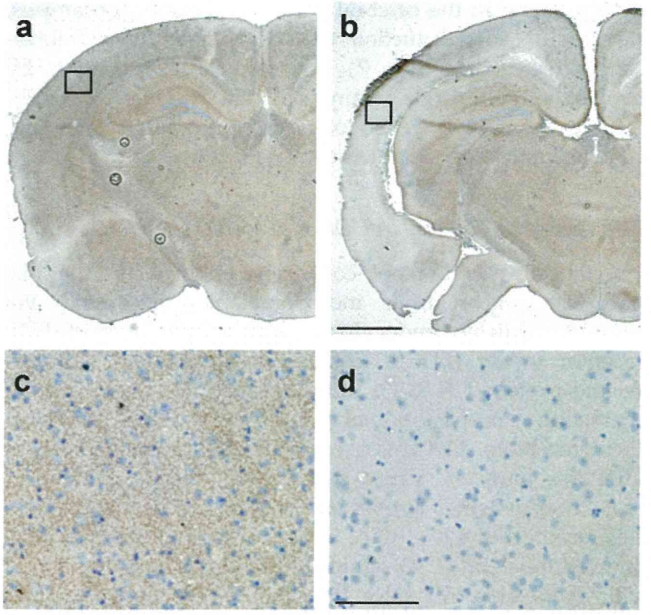

FIG. 7. Regional suppression of BACE1 protein by Toc-siBACE/HDL. **(a)** PBS-infused or **(b)** Toc-siBACE/HDL–infused brain sections were immunoperoxidase-stained for BACE1. Reduced DAB staining in the entorhinal, parietal cortex, and hippocampus is shown. Scale bar, 500 μm. **(c, d)** Panels show insets in **a** and **b**, respectively. Scale bar, 50 μm.

white matter regions, despite the similar level of Cy3 signals from the extracellular space (red) between WT and LDLR$^{-/-}$ mice, Cy3-positive areas in astrocytes as shown in merged yellow were decreased for LDLR$^{-/-}$ mice compared with WT mice (Fig. 8b). When normalized to the total GFAP-positive green area, the decrease in glial uptake of Toc-siBACE/HDL in LDLR$^{-/-}$ mice was statistically significant (Fig. 8c; WT vs. LDLR$^{-/-}$, 0.306 ± 0.082 vs. 0.096 ± 0.05, $p = 0.019$).

Discussion

The ability to direct a particular class of drugs to the brain has been desired for years, but the existence of the blood–brain barrier and the peculiar metabolism of the brain are major obstacles for drug delivery. In this study we developed a new and efficient method of delivering siRNA to the brain by conjugating it with α-tocopherol and HDL. Our vector system significantly lowered the dose of siRNA needed for silencing the target mRNA in the CNS.

Similar gene-silencing trials with ICV infusion of non-conjugated siRNA with chemical modifications have been reported (Senn *et al.*, 2005; Senechal *et al.*, 2007). The ICV infusion of free siRNA against dopamine receptor DDAR into the third ventricle of the mouse brain for 7 days could suppress the target mRNA by 60% with phenotypic change (Thakker *et al.*, 2004). Thakker *et al.*, (2004) reported the dose of free siRNA needed was as much as 3 μmol, whereas we found that just 3 nmol of Toc-siRNA with HDL could induce a target reduction in comparable degree by the same ICV infusion method. The *in vivo* knockdown using antisense oligonucleotides by its ICV infusion was also studied over the last two decades (Godfray and Estibeiro, 2003). Generally, ICV infused antisense oligonucleotides were more readily taken up by brain tissues than free siRNA, but their silencing efficacy is lower than free siRNA (Senn *et al.*, 2005). For example, 4.7 μmol of an ICV infusion of antisense oligonucleotides to superoxide dismutase 1 was needed to achieve 60% reduction of the target mRNA in the brain (Smith *et al.*, 2006). Roughly speaking, we could get a similar level of silencing effect in the brain with about a 1000-fold lower amount of siRNA with our method compared with ICV infused free siRNA or antisense oligonucleotides. The

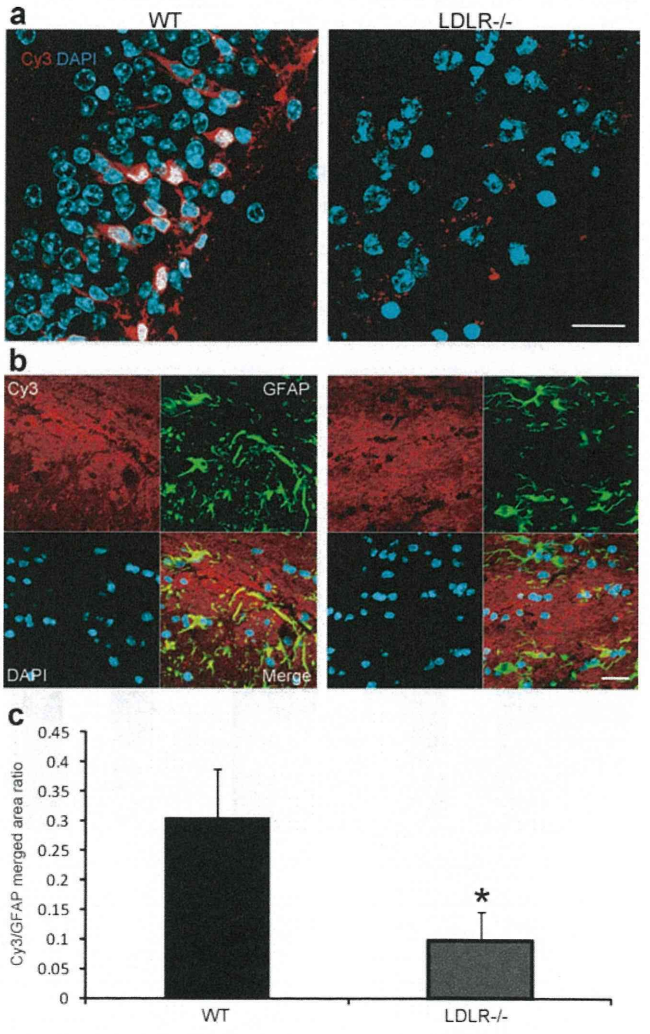

FIG. 8. Neuronal and glial uptake of Toc-siRNA/HDL mediated by LDL receptor. WT and LDLR$^{-/-}$ mice were intracerebroventricular (ICV) infused with Toc-siBACE/HDL for 7 days. **(a)** Confocal fluorescence observation revealed reduced uptake of Toc-siBACE/HDL in pyramidal neurons in the hippocampus CA3 of LDLR$^{-/-}$ mice compared with WT. Scale bar, 20 μm. **(b)** Immunofluorescence confocal observation for glial cells at corpus callosum of WT and LDLR$^{-/-}$ mice. Glial cells were detected by GFAP staining. Scale bar, 20 μm. **(c)** Bar graph shows Toc-siRNA/HDL uptake area ratio in glial cells from WT and LDLR$^{-/-}$ mice. GFAP and Cy3 positive yellow areas are divided by GFAP-positive green areas. WT, $n = 3$. LDLR$^{-/-}$, $n = 3$. Values represent mean $\pm$ SD. *$p = 0.019$, Student's t test.

direct intraparenchymal brain injection of naked siRNA (Querbes *et al.*, 2009), siRNA with cationic vector (Wang *et al.*, 2005), or cholesterol-conjugated siRNA (DiFiglia *et al.*, 2007) was also studied, but the distribution of siRNA was limited and the procedures were more invasive.

As the cause for our better RNAi effect, we think that our vector system utilizes the physiological lipid metabolism in the brain. The CNS has HDL-like particles that are synthesized mainly by astrocytes to mediate transport of lipids to neurons and glial cells (Vance *et al.*, 2005; Fünfschilling *et al.*, 2007). Since α-tocopherol is a highly lipophilic molecule and astrocytes express αTTP, we assumed that α-tocopherol is transferred from glial cells to neurons via the receptor-mediated pathway with HDL-like particles.

HDL-like particles in the brain contain ApoE as a major apolipoprotein, which is to be the ligand for the receptor-mediated endocytosis by LDLR and LRP1 in neurons (Rothe and Müller, 1991; Posse *et al.*, 2000). In addition, astrocytes also express LDLR and LRP-1 (LaDu, 2000; Rapp *et al.*, 2006) and internalize HDL-like particles. HDL-like particles and serum HDL are similar to each other in density and size, and both have ApoE and ApoA-1 (Pitas *et al.*, 1987). Since it was shown that rat sympathetic neurons can take up serum LDL and HDL as well as HDL-like particles via its LDLR (Rothe and Müller, 1991), we used serum HDL as a vector to deliver Toc-siRNA to neurons. Significant knockdown of endogenous BACE1 mRNA by ICV infusion of Toc-siRNA/HDL could not be obtained without binding to HDL, and moreover the delivery was much lower in $LDLR^{-/-}$ mouse brains. With these results, we believe that this vector system utilizes the physiological receptor-mediated lipid metabolism pathway of the brain, but not simple diffusion or macropinocytosis, to deliver siRNA. However, the uptake of Toc-siRNA/HDL in $LDLR^{-/-}$ mice was not completely diminished, suggesting that other lipoprotein receptors such as LRP1 or megalin, or another uptake mechanism of siRNA, such as a SID-1–mediated pathway in hepatocytes (Duxbury *et al.*, 2005), might contribute to the remaining uptake.

Although the delivery efficiency of siRNA by our vector system is better than previously reported, the reduction of the target mRNA of BACE1 was as much as 60% to 70%. Even partial reduction of BACE1, however, is suggested to have a dramatic effect on Alzheimer pathology in AD model mice with mutant amyloid precursor protein (APP). Single allele ablation caused only a 12% decrease in Aβ level, but nonetheless resulted in four- to fivefold fewer Aβ plaques (McConlogue *et al.*, 2007). Similarly, only 40% reduction of BACE1 protein by directly injected siRNA-expressing lentivirus significantly reduced AD pathology (Singer *et al.*, 2005). Additionally, duplication of the *APP* gene with a 1.5-fold gene dosage increase is known to cause familial AD (Blom *et al.*, 2008), suggesting that a 33% reduction of APP expression is enough to prevent the disease. Therefore, a more than 60% reduction of BACE1 with our vector system can be expected to reduce Aβ load and improve AD phenotype.

Together, we could achieve highly efficient gene silencing in the brain by ICV infusion of Toc-siRNA/HDL that should utilize the receptor-mediated physiological pathway. That resulted in lower doses by orders of magnitude than needed in previously reported methods for nucleotide delivery to the brain.

Acknowledgments

This work was supported by grants from the Japanese Society for the Promotion of Science (#20023010) and the Japan Foundation for Neuroscience and Mental Health (#2212070).

Author Disclosure Statement

The authors declare no competing financial interests.

References

Akinc, A., Goldberg, M., Qin, J., *et al.* (2009). Development of lipidoid-siRNA formulations for systemic delivery to the liver. Mol. Ther. 17, 872–879.

Akinc, A., Zumbuehl, A., Goldberg, M., *et al.* (2008). A combinatorial library of lipid-like materials for delivery of RNAi therapeutics. Nat. Biotechnol. 5, 561–569.

Blom, E.S., Viswanathan, J., Kilander, L., *et al.* (2008). Low prevalence of APP duplications in Swedish and Finnish patients with early-onset Alzheimer's disease. Eur. J. Hum. Genet. 2, 171–175.

DiFiglia, M., Sena-Esteves, M., Chase, K., *et al.* (2007). Therapeutic silencing of mutant huntingtin with siRNA attenuates striatal and cortical neuropathology and behavioral deficits. Proc. Natl. Acad. Sci. U. S. A. 43, 17204–17209.

Duxbury, M.S., Ashley, S.W., and Whang, E.E. (2005). RNA interference: a mammalian SID-1 homologue enhances siRNA uptake and gene silencing efficacy in human cells. Biochem. Biophys. Res. Commun. 2, 459–463.

Fan, Q., Iosbe, I., Asou, H., *et al.* (2001). Expression and regulation of apolipoprotein E receptors in the cells of the central nervous system in culture: A review. J. Am. Aging. Assoc. 24, 1–10.

Fünfschilling, U., Saher, G., Xiao, L., *et al.* (2007). Survival of adult neurons lacking cholesterol synthesis in vivo. BMC Neurosci. 8, 1.

Gao, S., Dagnaes-Hansen, F., Nielsen, E.J., *et al.* (2009). The effect of chemical modification and nanoparticle formulation on stability and biodistribution of siRNA in mice. Mol. Ther. 7, 1225–1233.

Godfray, J., and Estibeiro, P. (2003). The potential of antisense as a CNS therapeutic. Expert Opin. Ther. Targets. 3, 363–376.

Gohil, K., Oommen, S., Quach, H.T., *et al.* (2008). Mice lacking alpha-tocopherol transfer protein gene have severe alpha-tocopherol deficiency in multiple regions of the central nervous system. Brain Res. 1201, 167–176.

Goti, D., Balazs, Z., Panzenboeck, U., *et al.* (2002). Effects of lipoprotein lipase on uptake and transcytosis of low density lipoprotein (LDL) and LDL-associated alpha-tocopherol in a porcine in vitro blood-brain barrier model. J. Biol. Chem. 32, 28537–28544.

Hatch, F.T., and Lees, R.S. (1968). Practical methods for plasma lipoprotein analysis. Advan. Lipid Res. 6, 1–68.

Herz, J., and Chen, Y. (2006). Reelin, lipoprotein receptors and synaptic plasticity. Nat. Rev. Neurosci. 11, 850–859.

Hosomi, A., Goto, K., Kondo, H., *et al.* (1998). Localization of alpha-tocopherol transfer protein in rat brain. Neurosci. Lett. 3, 159–162.

Kao, S.C., Krichevsky, A.M., Kosik, K.S., and Tsai, L.H. (2004). BACE1 suppression by RNA interference in primary cortical neurons. J. Biol. Chem. 3, 1942–1949.

Kappus, H., and Diplock, A.T. (1992). Tolerance and safety of vitamin E: a toxicological position report. Free Radic. Biol. Med. 1, 55–74.

Kim, D.H., Behlke, M.A., Rose, S.D., *et al.* (2005). Synthetic dsRNA Dicer substrates enhance RNAi potency and efficacy. Nat. Biotechnol. 2, 222–226.

Kumar, P., Wu, H., McBride, J.L., *et al.* (2007). Transvascular delivery of small interfering RNA to the central nervous system. Nature 7149, 39–43.

LaDu, M.J. (2000). Apolipoprotein E receptors mediate the effects of beta-amyloid on astrocyte cultures. J. Biol. Chem. 43, 33974–33980.

Lima, W.F., Murray, H., Nichols, J.G., *et al.* (2009). Human Dicer binds short single-strand and double-strand RNA with high affinity and interacts with different regions of the nucleic acids. J. Biol. Chem. 4, 2535–2548.

Mardones, P., Strobel, P., Miranda, S., *et al.* (2002). Alpha-tocopherol metabolism is abnormal in scavenger receptor class B type I (SR-BI)-deficient mice. J. Nutr. 3, 443–449.

McConlogue, L., Buttini, M., Anderson, J.P., *et al.* (2007). Partial reduction of BACE1 has dramatic effects on Alzheimer plaque and synaptic pathology in APP Transgenic Mice. J. Biol. Chem. 282, 26326–26334.

Moschos, S.A., Williams, A.E., and Lindsay, M.A. (2007). Cell-penetrating-peptide-mediated siRNA lung delivery. Biochem. Soc. Trans. 4, 807–810.

Nishina, K., Unno, T., Uno, Y., *et al.* (2008). Efficient in vivo delivery of siRNA to the liver by conjugation of alpha-tocopherol. Mol. Ther. 4, 734–740.

Pfrieger, F.W. (2003). Cholesterol homeostasis and function in neurons of the central nervous system. Cell Mol. Life Sci. 6, 1158–1171.

Pitas, R.E., Boyles, J.K., Lee, S.H., *et al.* (1987). Lipoproteins and their receptors in the central nervous system. J. Biol. Chem. 29, 14352–14360.

Posse De Chaves, E.I., Vance, D.E., Campenot, R.B., *et al.* (2000). Uptake of lipoproteins for axonal growth of sympathetic neurons. J. Biol. Chem. 26, 19883–19890.

Qian, J., Morley, S., Wilson, K., *et al.* (2005). Intracellular trafficking of vitamin E in hepatocytes: the role of tocopherol transfer protein. J. Lipid Res. 10, 2072–2082.

Querbes, W., Ge, P., Zhang, W., *et al.* (2009). Direct CNS Delivery of siRNA Mediates Robust Silencing in Oligodendrocytes. Oligonucleotides 1, 23–30.

Rapp, A., Gmeiner, B., and Hüttinger, M. (2006). Implication of apoE isoforms in cholesterol metabolism by primary rat hippocampal neurons and astrocytes. Biochimie 5, 473–483.

Rigotti, A. (2007). Absorption, transport, and tissue delivery of vitamin E. Mol. Aspects Med. 5–6, 423–436.

Rothe, T., and Müller, H.W. (1991). Uptake of endoneurial lipoprotein into Schwann cells and sensory neurons is mediated by low density lipoprotein receptors and stimulated after axonal injury. Neurochem. 6, 2016–2025.

Rozema, D.B., Lewis, D.L., Wakefield, D.H., *et al.* (2007). Dynamic PolyConjugates for targeted in vivo delivery of siRNA to hepatocytes. Proc. Natl. Acad. Sci. USA. 32, 12982–12987.

Senechal, Y., Kelly, P.H., Cryan, J.F., *et al.* (2007). Amyloid precursor protein knockdown by siRNA impairs spontaneous alternation in adult mice. J. Neurochem. 6, 1928–1940.

Senn, C., Hangartner, C., Moes, S., *et al.* (2005). Central administration of small interfering RNAs in rats: a comparison with antisense oligonucleotides. Eur. J. Pharmacol. 1–3, 30–37.

Singer, O., Marr, R.A., Rockenstein, E., *et al.* (2005). Targeting BACE1 with siRNAs ameliorates Alzheimer disease neuropathology in a transgenic model. Nat. Neurosci. 10, 1343–1349.

Smith, R.A., Miller, T.M., Yamanaka, K., *et al.* (2006). Antisense oligonucleotide therapy for neurodegenerative disease. J. Clin. Invest. 8, 2290–2296.

Thakker, D.R., Natt, F., Hüsken, D., *et al.* (2004). Neurochemical and behavioral consequences of widespread gene knockdown in the adult mouse brain by using nonviral RNA interference. Proc. Natl. Acad. Sci. USA. 49, 17270–17275.

Vance, J.E., Hayashi, H., and Karten, B. (2005). Cholesterol homeostasis in neurons and glial cells. Semin. Cell Dev. Biol. 2, 193–212.

Wang, Y.L., Liu, W., Wada, E., *et al.* (2005). Clinico-pathological rescue of a model mouse of Huntington's disease by siRNA. Neurosci. Res. 3, 241–249.

Wolfrum, C., Shi, S., Jayaprakash, K.N., *et al.* (2007). Mechanisms and optimization of in vivo delivery of lipophilic siRNAs. Nat. Biotechnol. 10, 1149–1157.

Yokota, T., Igarashi, K., Uchihara, T., *et al.* (2001). Delayed-onset ataxia in mice lacking alpha-tocopherol transfer protein: model for neuronal degeneration caused by chronic oxidative stress. Proc. Natl. Acad. Sci. USA. 26, 15185–15190.

Yu, L., Tan, M., Ho, B., *et al.* (2006). Determination of critical micelle concentrations and aggregation numbers by fluorescence correlation spectroscopy: aggregation of a lipopolysaccharide. Anal. Chim. Acta 1, 216–225.

Zimmermann, T.S., Lee, A.C., Akinc, A., *et al.* (2006). RNAi-mediated gene silencing in non-human primates. Nature 441, 111–114.

Address correspondence to:
Takanori Yokota
Department of Neurology and Neurological Science
Tokyo Medical and Dental University
1-5-45 Yushima
Bunkyo-ku
Tokyo 113-8519
Japan

E-mail: tak-yokota.nuro@tmd.ac.jp

Received for publication November 7, 2010;
accepted after revision December 17, 2010.

Published online: December 17, 2010.

Biochemical and Biophysical Research Communications 405 (2011) 204–209

Contents lists available at ScienceDirect

Biochemical and Biophysical Research Communications

journal homepage: www.elsevier.com/locate/ybbrc

Intraperitoneal AAV9-shRNA inhibits target expression in neonatal skeletal and cardiac muscles

Azat Mayra [a], Hiroyuki Tomimitsu [a], Takayuki Kubodera [a], Masaki Kobayashi [a], Wenying Piao [a], Fumiko Sunaga [a], Yukihiko Hirai [b], Takashi Shimada [b], Hidehiro Mizusawa [a], Takanori Yokota [a,*]

[a] Department of Neurology and Neurological Science, Graduate School, Tokyo Medical and Dental University, 1-5-45 Yushima, Bunkyo-ku, Tokyo 113-8519, Japan
[b] Department of Biochemistry and Molecular Biology, Nippon Medical School, 1-1-5 Sendagi, Bunkyo-ku, Tokyo 113-8602, Japan

ARTICLE INFO

Article history:
Received 24 November 2010
Available online 8 January 2011

Keywords:
shRNA
AAV9
Neonatal

ABSTRACT

Systemic injections of AAV vectors generally transduce to the liver more effectively than to cardiac and skeletal muscles. The short hairpin RNA (shRNA)-expressing AAV9 (shRNA-AAV9) can also reduce target gene expression in the liver, but not enough in cardiac or skeletal muscles. Higher doses of shRNA-AAV9 required for inhibiting target genes in cardiac and skeletal muscles often results in shRNA-related toxicity including microRNA oversaturation that can induce fetal liver failure.

In this study, we injected high-dose shRNA-AAV9 to neonates and efficiently silenced genes in cardiac and skeletal muscles without inducing liver toxicity. This is because AAV is most likely diluted or degraded in the liver than in cardiac or skeletal muscle during cell division after birth. We report that this systemically injected shRNA-AAV method does not induce any major side effects, such as liver dysfunction, and the dose of shRNA-AAV is sufficient for gene silencing in skeletal and cardiac muscle tissues. This novel method may be useful for generating gene knockdown in skeletal and cardiac mouse tissues, thus providing mouse models useful for analyzing diseases caused by loss-of-function of target genes.

1. Introduction

Since the discovery that RNA interference (RNAi), mediated by small interference RNA (siRNA), can inhibit target gene expression, RNAi has become the standard tool for sequence-specific knockdown of gene expression in molecular biology [1]. RNAi biology utilizes short hairpin RNA (shRNA) usually expressed from plasmid or viral vectors. Base-pair stems and a loop region characterize shRNAs. Different types of promoters can be used for shRNA expression and, therefore, various knockdown models using tissue- or cell-specific promoters for target genes can be generated [2].

Another small RNA, microRNA (miRNA), is known to bind endogenous non-protein coding genes, with the precursors of miRNAs being hairpin structures similar to shRNAs. The miRNA and shRNA are known to utilize the common pathways of exportin-5 for nuclear export and the processing by Dicer and Argonaute family proteins in the cytoplasm. As these processes are competed for by miRNA and shRNA, a high level of shRNA expression could interfere with miRNA maturation and cause damage to the cells [1,4]. From these view points, properly designed and expressed shRNAs are necessary to establish knockdown models of chronic diseases that are both acquired and inherited.

For generating in vivo models of disease by using shRNAs, the main constraint is the difficulty in delivering the shRNA to the target tissues. Delivery of gene vectors to local skeletal muscles and cardiac muscle has been achieved by direct intramuscular injection or by local blood perfusion with nonviral and viral vectors, including plasmid DNA and adeno-associated virus (AAV) [5,6]. A number of AAV serotype vectors are available, with AAV1, 6, 8 and 9 being reported to efficiently express the transgenes in skeletal and cardiac muscles [7–11]. However, there are only a few reports claiming that systemic AAV-shRNA vector injection can significantly inhibit target genes in skeletal muscle. One paper showed a significant reduction of the target gene in skeletal muscle and liver by using tail vein injection of AAV type 6 [12], yet liver function was not examined. In our preliminary study, intravenously administered high dose AAV8- or AAV9-shRNA (1×10^{12} v.g./mouse) achieved substantial inhibition of the target gene in the liver, but induced severe liver damage without sufficient gene silencing in the skeletal muscle itself. Intraperitoneal administration of AAV vectors in neonatal mice showed significantly higher expression of target genes than in adult mice. Moreover, using systemic administration of AAV vectors in neonatal mice, target genes can be delivered to neurons and cardiac and skeletal muscle more efficiently [10,13–16]. In this study, we injected AAV9-shRNA intraperitoneally to neonates and sufficiently inhibited the target genes in skeletal and cardiac muscles without detecting any side effects, including liver damage.

* Corresponding author. Fax: +81 3 5803 0169.
E-mail address: tak-yokota.nuro@tmd.ac.jp (T. Yokota).

0006-291X/$ - see front matter © 2011 Elsevier Inc. All rights reserved.
doi:10.1016/j.bbrc.2011.01.009

2. Materials and methods

2.1. Construction of the anti-SOD1 shRNA AAV9 vector

We prepared the anti-SOD1 shRNA cassette as previously reported [17]. The anti-SOD1 shRNA cassette was cloned downstream of the polymerase III (PolIII) human U6 promoter in the AAV vector (Stratagene, La Jolla, CA, USA) plasmid (Fig. 1). The silencing efficiency of the anti-SOD1 shRNA sequence was verified using several cultured cell lines and transgenic mice expressing the anti-SOD1 shRNA, as previously described [3]. Human growth hormone polyadenylation (hGH poly A) cassette (Stratagene) was inserted downstream of the shRNA sequence in the vector for the titration assay of the vector by quantitative real-time PCR (Fig. 1).

2.2. Production and titration of the anti-SOD-shRNA AAV9 vector

The recombinant viral vector was produced according to the three-plasmid transfection protocol using the calcium phosphate method [18]. Human embryonic kidney cultured cells (HEK 293 cells) at approximately 70% confluence were transfected with the AAV9 packaging plasmid, pRep2/Cap9 (a kind gift from Wilson J), adenovirus Helper plasmid (Stratagene), and the pAAV-anti-SOD1-shRNA plasmid, at a ratio of 1:1:1. At 6 h post-transfection the medium was replaced with fresh culture medium containing 2% fetal bovine serum (Sigma, St. Louis, MO, USA), and the cells were cultured for 48 h at 37 °C. After the incubation, the cells were harvested and pelleted by centrifugation at 4000 rpm. The pellets were then resuspended in Tris–HCl (pH 8.5), and after treatment with 5% sodium deoxycholate for 30 min at 37 °C, the cells were subjected to three freeze–thaw cycles. The cell suspension was treated with Benzonase (Merck, Darmstadt, Denmark), followed by the process of ammonium sulfate deposition using $(NH_4)_2SO_4$ (pH 8.5). Cell pellets contained the AAV dissolved in phosphate buffered saline (PBS), and the viral solution was layered with Optiprep (Axis-shield, Oslo, Norway). After centrifugation of the solution at 52,000 rpm for 17 h at 15 °C, the viral fractions were collected from the bottom of the gradient.

Genome titers of the AAV vectors were determined by quantitative PCR using the TaqMan system. The following primers and probes targeting the polyA signal were used: 5′-CAGGCTGGTC TCCAACTCCTC-3′ and 5′-GCAGTGGTTCACGCCTGTAA-3′ served as the primer set, and 5′-TACCCACCTTGGCCTC-3′ served as the probe.

2.3. Animals

All of the animal procedures were performed in accordance with the protocols approved by the Animal Experiment Committee of Tokyo Medical and Dental University (#0100101). All of the ICR mice were obtained from Orient Yeast Co. Ltd. (Tokyo, Japan). Postnatal day-1 ICR mice were injected intraperitoneally with 5×10^{11} vector genome per gram (v.g./g) of the anti-SOD1 shRNA AAV9 vector ($n = 4$). Non-injected littermates were used as the control group ($n = 4$). The body weights of the mice were measured chronologically. At 4 weeks after the injection, all of the mice were euthanized after performing the rotarod tests. Blood, skeletal muscles (quadriceps and hamstrings), cardiac muscle, and liver tissues were collected for analysis.

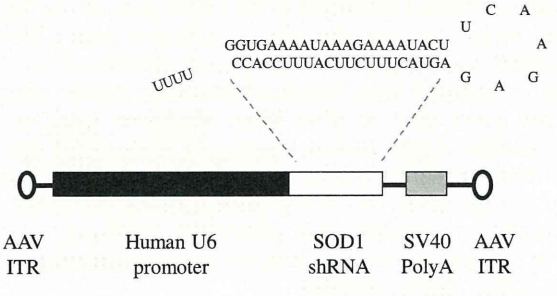

Fig. 1. Construction of the anti-SOD1 shRNA AAV9 vector. The anti-SOD1 shRNA expression AAV9 vector including an anti-SOD1 shRNA between the polymerase III human U6 promoter and hGH polyA cassette.

2.4. Rotarod test

The rotarod test was performed using the accelerating Rotarod (Ugo Basile Biological Research Apparatus, Varese, Italy). The 4-week-old mice in both groups were placed on the rod (3 cm diameter) in four trials each day, for a series of 4 days. Each trial lasted up to a maximum of 10 min; the time spent on the rod without falling was recorded. The average time of each group was calculated and statistical significance was assessed by one-way ANOVA. Significance was defined as $p < 0.05$.

2.5. Northern blotting analysis of shRNA

The RNAs were derived from quadriceps, hamstrings, cardiac muscle, and liver using MirVana (Ambion, Austin, TX, USA). Three micrograms of RNA derived from each tissue were separated on 18% polyacrylamide-urea gels, and transferred to Hybond-N+ membranes (GE Healthcare, Piscataway, UK). The blots were hybridized with a probe against the antisense sequence of the shRNA. The probe sequence was 5′-GGTGGAAATGAAGAAAGTAC-3′. The probe was labeled using DIG Oligonucleotide 3′-End Labeling Kit 2nd Generation (Roche, Penzberg, Germany). The signal was visualized using the Gene Images CDP-star detection kit (GE Healthcare).

2.6. Measurement of RNA reduction by quantitative RT-PCR

Total RNAs were extracted from the collected tissues using Isogen (Nippon Gene, Toyama, Japan). DNase-treated total RNAs (0.5 μg) were reverse transcribed using SuperScript III Reverse Transcriptase (Invitrogen, Carlsbad, CA, USA). The cDNAs were amplified by the quantitative TaqMan system on a Light Cycle 480 Real-Time PCR Instrument (Roche), according to the manufacturer's protocol. SOD1 mRNA expression level in each tissue was measured using the primers and probe designed as follows: Forward primer: 5′-GGTGCAGGGAACCATCCA-3′, reverse primer: 5′-CCCATGCTGGCCTTCAGT-3′, and the probe: 5′-AGGCAAGCGGTGAA CCAGTTGTGTTG-3′. In order to normalize the RT-PCR values, the cDNAs were also amplified quantitatively with the TaqMan primers and the probe sets for GAPDH (Applied Biosystems, Warrington, UK). The ratio of SOD1 mRNA expression level to GAPDH expression was calculated to estimate the shRNA silencing efficiency. Significant differences between the two groups were calculated with the Welch's *T*-test.

2.7. Western blotting

Protein samples were extracted from the liver, hamstrings and cardiac muscles. The tissues were homogenized in cold homogenization buffer containing 0.1% sodium dodecylsulfate (SDS), 1% sodium deoxycholate, 1% Triton X-100, and 1 mM phenylmethylsulfonyl fluoride, together with a protein inhibitor cocktail (Roche). Eight micrograms of the extracted protein of each sample was mixed with laemmli sample buffer (BioRad, Hercules, CA, USA), denatured at 95 °C for 5 min, and separated on a 15% SDS–PAGE gel. The separated proteins were transferred to a polyvinylidene difluoride membrane (BioRad), and incubated with the specific primary antibodies, rabbit anti-SOD1 antibody (StressGen Biotechnologies, Victoria, British Columbia, Canada) and mouse anti-GAPDH

monoclonal antibody (Biodesign, Saco, ME, USA). After incubation, the membrane was rinsed and incubated with 0.1% horseradish peroxidase conjugated secondary antibodies, goat anti-rabbit HRP IgG and goat anti-mouse HRP IgG (Thermo Science, Rockford, IL, USA). Protein–antibody interactions were visualized using the supersignal west femto maximum sensitivity substrate (Thermo Science).

2.8. Pathological examinations

The skeletal muscles were frozen rapidly in liquid-nitrogen-cooled isopentane, and the liver and cardiac muscles were fixed in 10% formalin and embedded in paraffin. Ten-microgram frozen sections of skeletal muscles and 5-μm paraffin sections of liver and cardiac muscle were processed for hematoxylin and eosin staining.

2.9. Blood chemistry examinations

The sera were prepared from blood samples of the mice. In order to evaluate liver and muscle function, serum alanine aminotransferase (ALT), aspartate aminotransferase (AST), alkaline phosphatase (ALP), lactate dehydrogenase (LDH), total bilirubin (T-BIL), albumin (ALB), total protein (TP), and creatine kinase (CK) were measured (Oriental Yeast Co. Ltd., Tokyo, Japan). Statistically significant differences between the injected group and the control group were calculated by the Welch's *T*-test.

3. Results

3.1. Growth and health status of the injected mice

After the mice were injected with anti-SOD1 shRNA AAV9, they were raised together with their littermate controls for 4 weeks. The body weights of the injected mice and their littermate controls were similar (Fig. 2A). In the accelerating rotarod tests, there were no significant differences in motor function between the injected mice and littermate controls (Fig. 2B). At the end of the experimental period, the mice were dissected and showed no morphological abnormalities such as hepatomegaly, cardiomegaly, ascites, pleural effusion, edema, body fluid retention, or adhesion of organs.

3.2. Tissue expression of anti-SOD1 shRNA

Expression of anti-SOD1 shRNA in the liver, quadriceps, hamstrings and cardiac muscles was demonstrated by northern blot analysis (Fig. 3A). Fifty-four nucleotides (nt) of shRNA were not detected in these tissues (data not shown); however, a 21-nt antisense strand of siRNA was detected. This finding clearly indicates that the expressed anti-SOD1 shRNA was almost completely processed by Dicer. The expression level of the antisense siRNA was robust in cardiac and hamstring muscles, but surprisingly, much less in quadriceps muscles. Importantly, expression of siRNA was not detected in the liver.

3.3. The inhibitory effect of SOD1 mRNA

Quantitative RT-PCR showed that the expression level of SOD1 mRNA in the cardiac and hamstrings muscles of the injected mice was significantly reduced in comparison with those of the littermate controls. Using this method of injection, we observed approximately 80% reduction of SOD1 mRNA in the cardiac muscles and 65% reduction in the hamstrings. However, reduction of SOD1 mRNA in the quadricep muscles and liver were mild or absent (Fig. 3B). Effective suppression of the SOD1 gene was also confirmed at the protein level by Western blot analysis. Expression of the SOD1 protein was markedly reduced in the cardiac and hamstring muscles, but reduction in the liver was not clear (Fig. 3C).

3.4. Pathological examinations

HE staining of the injected mouse specimens showed no inflammatory changes in cardiac and skeletal muscles or in the liver (Fig. 4). In the hamstring muscle, we found no abnormal fibers such as small angular fibers, necrotic or regenerative muscle fibers. In the cardiac muscle, abnormal findings such as interstitial proliferation and muscle fiber degeneration were not seen. In the liver pathology, we found no structural abnormalities such as hepatic lobules.

3.5. Blood chemistry examinations

Serum AST, ALT, ALP, LDH, CK, ALB and TP values in both groups are shown in Table 1. Serum AST, ALT and LDH were increased

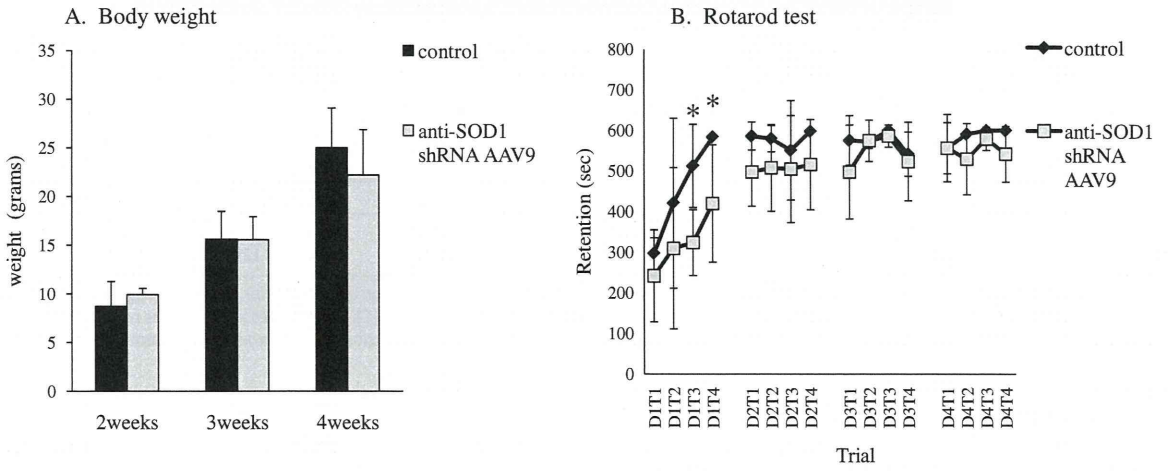

Fig. 2. Mouse growth and movement ability. (A) During the 4-week experimental period, none of the anti-SOD1 shRNA AAV9 vector-injected mice showed any significant differences in body weight compared with the littermate controls. Data are presented as the mean with SD ($n = 4$ for each group, $p > 0.05$). (B) In the accelerating rotarod test 4 weeks after injection of the anti-SOD1 shRNA AAV9 vector, all of the mice could perform the task similar to that of the littermate controls. Each mouse was trained in four trials each day (T1–T4), for a series of 4 days (D1–D4). Except for the third and fourth test of the first day (in the D1T3 $p = 0.025$, in the D1T4 $p = 0.048$), there was no significant difference between the injected mouse group and the littermate control group. Data are presented as the mean with SD ($n = 4$ for each group, $p > 0.05$).